



Jason-3 Products Handbook

References:

CNES : SALP-MU-M-OP-16118-CN

EUMETSAT : TBD

JPL : TBD

NOAA/NESDIS : TBD

Issue: 2 rev 2

Date: November 16th, 2022



Chronology Issues:

Issue:	Date:	Reason for change:
1rev0	July 9 th , 2012	Initial Issue of the document (related to CNES internal change requests SALP-FT-8044, SALP-FT-8377 and SALP-FT-8477)
1rev1	June 1 st , 2015	New release before launch to take into account: <ul style="list-style-type: none"> • New 4-partners approved logo on front page. • Modification of the AVISO+ contact/address. • Update of NRT & offline data access for NOAA. • 4-partner change request TP4-FT-383: Documentation update w.r.t orbit GDR-E standard modification for JASON-3.
1rev2	February 12, 2016	TP4-FT-446 <ul style="list-style-type: none"> • Update of launch date, first cycle. • Update of information about BUFR encoding software. • Details added in several paragraphs.
1rev3	August 23, 2016	SALP-FT-10562 <ul style="list-style-type: none"> • Modification of reference orbit parameters which are aligned with actual parameters of previous Jason missions (“historical” orbit)
1rev4	January 16, 2017	SALP-FT-10764 Modification of GDR latency after OSTST 2016 recommendation. Latency extended from 60 to 90 days in order to allow cold sky calibration processing and use in radiometer calibrations.
1rev5	September 17, 2018	SALP-FT-11270 Upgrade from POE-E to POE-F on Jason-3
1rev6	July 23, 2019	SALP-FT-10176: Add reference to Altitude Grid in xref_meteorological_files SALP-FT-11281: Implementation of a DORIS + GPS solutions for MOE
2rev0	Sept 21, 2020	Issue for Jason-3 GDR-F Standard : SALP-FT-10789, SALP-FT-11268, SALP-FT-1905, SALP-FT-12055, SALP-FT-12056, SALP-FT-12063, SALP-FT-12080, SALP-FT-12160, SALP-FT-12237, SALP-FT-12320, SALP-FT-11435
2rev1	June 21, 2021	SALP-FT-12933 : GDR-F : processing Baseline 1.02 : precisions on model Dry Tropo, model Wet tropo and atmospheric attenuation.
2rev2	November 16th, 2022	SALP-FT-13225 : Jason-3 repositionning to reach interleaved orbit interleaved orbit



Jason-3 Products Handbook

Iss :2.2 - date : Nov. 16th , 2022



i.2



People involved in this issue:

F. BIGNALET-CAZALET	CNES	
N. PICOT	CNES	
S. DESAI	NASA/JPL	
R. SCHARROO	EUMETSAT	
A. EGIDO	NOAA	



List of tables and figures

List of tables:

Table 1 : Differences between Auxiliary Data for O/I/GDR Products	1
Table 2 : Summary of operational, interim, and final geophysical data record products (O/I/GDR) from Jason-3.	2
Table 3 : Summary of error budget at the end of the verification phase of Jason-2	11
Table 4 : Main features of the Jason-3 satellite	14
Table 5 : Mean classical orbit elements	18
Table 6 : Orbit auxiliary data	18
Table 7 : Equator Crossing Longitudes (in order of Pass Number)	21
Table 8 : Equator Crossing Longitudes (in order of Longitude)	22
Table 9 : Equator Crossing Longitudes (in order of Pass Number)	23
Table 10 : Equator Crossing Longitudes (in order of Longitude)	24
Table 11 : Models and standards (Jason-3 Product Version "T")	32
Table 12 : Models and standards (Jason-3 Product Version "D")	33
Table 13: Models and standards (Jason-3 Product Version "F")	35
Table 14. POE-E/POE-F orbit standard	38
Table 15 : MSS_CNES-CLS15 model characteristics	39
Table 16 : MDT_CNES-CLS18 model characteristics	41
Table 17 : Recommended editing criteria	46
Table 18 : Recommended filtering criteria	46
Table 19 : List of classes defined for Jason-3 waveforms	59
Table 20 : Main characteristics of (O)(I)GDR products	65

List of figures:

Figure 1 : Altimetric distances - Altitude, Range and Height	5
Figure 2 : Main components of the Jason-3 satellite	13
Figure 3 : Jason-3 Poseidon-3 Instrument	14
Figure 4 : Jason-3 AMR Instrument and Antenna	15
Figure 5 : Jason-3 DORIS Receiver Antenna and Instrument	16
Figure 6 : Jason-3 Laser Reflector Array	16
Figure 7 : Jason-3 Precision GPS Receiver	16
Figure 8 : Jason-3 CARMEN-3 Instrument	17
Figure 9 : Jason-3 LPT	17
Figure 10 : T/P, Jason-1 (reference orbit), OSTM/Jason-2 and Jason-3 ground track coverage every 10 days	18
Figure 11 : Mean Sea Surface MSS_CNES-CLS15.	39
Figure 12 : Mean Dynamic Topography MDT_CNES-CLS18	41



Figure 13 : EGM2008 geoid	42
Figure 14 : Data set availability per product	67

Applicable documents / reference documents

- AD 1 : Jason-3 System Requirements
TP4-JO-STB-44-CNES
- AD 2 : Jason-3 Mission Requirements Documents
TP4-JO-SP-52-CNES
- AD 3 : Algorithm Definition, Accuracy and Specification - Bibli_Alti : Altimeter Level
1b Processing
SALP-ST-M2-EA-15596-CN
- AD 4 : Algorithm Definition, Accuracy and Specification - Bibli_Alti : Radiometer Level
1b Processing
SALP-ST-M2-EA-15597-CN
- AD 5 : Algorithm Definition, Accuracy and Specification - Bibli_Alti : Altimeter Level 2
Processing
SALP-ST-M2-EA-15598-CN
- AD 6 : Algorithm Definition, Accuracy and Specification - Bibli_Alti : Off-Line Control
Processing
SALP-ST-M2-EA-15599-CN
- AD 7 : Algorithm Definition, Accuracy and Specification - Bibli_Alti :
Altimeter/Radiometer Verification Processing
SALP-ST-M2-EA-15703-CN
- AD 8 : Algorithm Definition, Accuracy and Specification - Bibli_Alti : Mechanisms
SALP-ST-M2-EA-15600-CN
- AD 9 : SALP Products Specification - Volume 30 : Jason-3 User Products
SALP-ST-M-EA-16122-CN

- RD 1 : OSTM/Jason-2 Products Handbook
SALP-MU-M-OP-15815-CN



Contents

- 1. Introduction 1**
 - 1.1. Overview of the Jason-3 product family 1**
 - 1.1.1. Product contents 2
 - 1.1.2. Filename conventions 2
 - 1.2. Handbook Overview 4**
 - 1.3. Document reference and contributors 4**
 - 1.4. Conventions 4**
 - 1.4.1. Vocabulary 4
 - 1.4.1.1. Altimetric distances 4
 - 1.4.1.2. Orbits, Revolutions, Passes, and Repeat Cycles 5
 - 1.4.1.3. Reference Ellipsoid 6
 - 1.4.2. Correction Conventions 6
 - 1.4.3. Time Convention 6
 - 1.4.4. Unit Convention 6
 - 1.4.5. Flagging and Editing 6
- 2. Jason-3 Mission Overview 7**
 - 2.1. Background 7**
 - 2.2. Introduction to Jason-3 Mission 7**
 - 2.2.1. Mission overview 7
 - 2.2.2. Mission objectives 8
 - 2.2.3. Mission partnership 8
 - 2.2.4. Mission launch 10
 - 2.3. Jason-3 Requirements 10**
 - 2.3.1. Accuracy of Sea-level Measurements 10
 - 2.3.2. Sampling Strategy 11
 - 2.3.3. Tidal Aliases 11
 - 2.3.4. Duration and coverage 11
 - 2.4. Satellite Description 12**
 - 2.4.1. Satellite Characteristics 14
 - 2.4.2. Sensors 14
 - 2.4.2.1. Poseidon-3B Altimeter 14
 - 2.4.2.2. Advanced Microwave Radiometer (AMR) 14



2.4.2.3. DORIS System	15
2.4.2.4. Laser Reflector Array	16
2.4.2.5. GPS Receiver	16
2.4.2.6. CARMEN-3 Radiation Detectors.....	16
2.4.2.7. LPT Detection Unit	17
2.4.3. Orbit	17
2.4.3.1. Repetitive orbit on historical ground track (January 2016 - April 2022).....	17
2.4.3.1.1. Equator Crossing Longitudes (in order of Pass Number)	20
2.4.3.1.2. Equator Crossing Longitudes (in order of Longitude)	21
2.4.3.2. Repetitive orbit on interleaved orbit (April 2022-nowadays)	22
2.4.3.2.1. Equator Crossing Longitudes (in order of Pass Number)	22
2.4.3.2.2. Equator Crossing Longitudes (in order of Longitude)	23
2.4.4. The Jason-3 Project Phases	24
2.4.4.1. The verification phase	24
2.4.4.2. The operational (routine and long-term CALVAL activities)	24
2.5. Data Processing and Distribution	25
2.5.1. Access to NRT data	26
2.5.2. Access to off-line data	26
2.5.3. Documentation	26
2.6. Access to data via NOAA.....	27
2.6.1. Access to NRT data	27
2.7. Access to data via EUMETSAT	27
2.7.1. NRT data access.....	27
2.7.2. Access to archived data	28
2.8. Access to OGDR-BUFR files data on GTS.....	29
2.9. CNES data distribution.....	29
2.9.1. Details of off line data access via CNES.....	29
3. Product evolution history.....	30
3.1. Models and Standards History	30
3.1.1. Models and Standards on Version "T" products	30
3.1.2. Models and Standards on Version "D" products	32
3.1.3. Models and standards on Version "f" Products	33
3.2. Models and Editing on Version "F" Products	35
3.2.1. Orbit models	35
3.2.2. Mean Sea Surface	39



3.2.2.1. MSS_CNES-CLS15	39
3.2.2.2. MSS_DTU-2018	40
3.2.3. Mean Dynamic Topography	41
3.2.4. Geoid	41
3.2.5. Bathymetry	42
3.2.6. Ocean Tides	42
3.2.6.1. GOT4.10c Ocean Tide Model	43
3.2.6.2. FES2014b Ocean Tide Model	43
3.2.7. Sea Surface Height Bias Recommendation	44
3.2.8. Surface Classification Map	45
3.2.9. Coastal Distance & Angle of Approach to Coast	45
3.2.10. Global Slope Correction	45
3.2.11. Data Editing Criteria	45
4. Using the (O)(I)GDR data	47
4.1. Overview	47
4.2. Typical computation from altimetry data.....	47
4.2.1. Corrected Altimeter Range	48
4.2.2. Sea Surface Height and Sea Level Anomaly.....	48
4.2.2.1. Tide Effects	49
4.2.2.2. Geophysical Surface - Mean Sea Surface or Geoid	51
4.2.3. Mean Sea Surface and Adjustment of the Cross Track Gradient	51
4.2.4. Total Electron Content from Ionosphere Correction	52
4.2.5. Range Compression.....	52
5. Altimetric data.....	54
5.1. Precise Orbits	54
5.2. Altimeter Range.....	54
5.3. Geoid.....	54
5.4. Mean Sea Surface	55
5.5. Mean Dynamic Topography	55
5.6. Geophysical Corrections.....	55
5.6.1. Troposphere (Dry and Wet)	55
5.6.1.1. Dry Troposphere	55
5.6.1.2. Wet Troposphere	56
5.6.2. Atmospheric Attenuation	57



5.6.3. Ionosphere	57
5.6.4. Ocean Waves (sea state bias)	57
5.7. Rain Flag.....	58
5.8. Ice Flag	58
5.9. Waveform Classification	59
5.10. Tides.....	60
5.10.1. Geocentric Ocean Tide	60
5.10.2. Long period Ocean Tide	60
5.10.3. Solid Earth Tide	61
5.10.4. Pole Tide	61
5.10.5. Internal Tide	62
5.11. Ocean response to atmospheric forcing	62
5.11.1. Inverted Barometer Correction	62
5.11.2. Dynamic Atmospheric Correction	63
5.12. Sigma 0.....	63
5.13. Wind Speed.....	63
5.14. Bathymetry Information	64
6. Data description	65
6.1. (O)(I)GDR content.....	65
6.2. Datasets	66
6.3. Product Description	67
6.4. Software	67
6.4.1. Software provided with netCDF : “ncdump”	67
6.4.2. Additional general software	68
6.4.2.1. ncbrowse	68
6.4.2.2. netCDF Operator (NCO).....	68
6.4.3. Additional specific software: “BRAT”	68
6.5. OGDR BUFR product.....	68
Annexe A - References	70
Annexe B - List of acronyms	73
Annexe C - Contacts.....	75



Jason-3 Products Handbook

Iss :2.2 - date : Nov. 16th , 2022



i.10





1. Introduction

Jason-3 is a follow-on mission to OSTM/Jason-2. The satellite is named after the leader of the Argonauts' famous quest to recover the Golden Fleece. The Jason-3 mission takes over and continues the TOPEX/Poseidon, Jason-1 and OSTM/Jason-2 missions. While the TOPEX/Poseidon and Jason-1 missions were conducted under a cooperation between the French Space Agency, "Centre National d'Etudes Spatiales" (CNES) and the United States National Aeronautics and Space Administration (NASA), Jason-3, alike OSTM/Jason-2, involves CNES, NASA and 2 additional partners: the European Organisation for the Exploitation of Meteorological Satellites (EUMETSAT) and the National Oceanic and Atmospheric Administration (NOAA) in order to facilitate the transition towards a fully operational altimetry mission, able to satisfy the data timeliness and reliability requirements of operational applications.

1.1. Overview of the Jason-3 product family

The purpose of this document is to assist users of the Jason-3 products (Operational Geophysical Data Record: OGDR, Interim Geophysical Data Record: IGDR, and Geophysical Data Record: GDR) by providing a comprehensive description of product content and format. We will so refer to (O)(I)GDR in this document when the information is relevant for all the products.

(O)(I)GDR products are identical except for the following differences regarding the auxiliary data used in the processing:

Auxiliary Data	Impacted Parameter	OGDR	IGDR	GDR
Orbit	Satellite altitude, Doppler correction, ...	DORIS Navigator	Preliminary (MOE using DORIS data and/or GPS data*)	Precise (POE using DORIS and/or Laser and/or GPS data)
Meteo Fields	Dry/wet tropospheric corrections, U/V wind vector, Surface pressure, Inverted barometer correction, ...	Predicted	Restituted	
	Waves	Not Available	MFWAM	
Pole Location	Pole tide height	Predicted		Restituted
Mog2D	HF ocean dealiasing correction	Predicted	Preliminary	Precise
GIM	Ionosphere correction	Not available	Available	
Radiometer antenna temperatures coeff.	Wet tropospheric correction, Sigma0 rain attenuation, ...	Preliminary		Precise (accounting for radiometer calibration)

Table 1 : Differences between Auxiliary Data for O/I/GDR Products

GDR products, unlike OGDR and IGDR products, are fully validated products.

* MOE uses only DORIS data before February 12th, 2019 and DORIS+GPS data afterwards




1.1.1. Product contents

The Level-2 products from this mission comprise a family of nine different types of geophysical data records (GDRs). As illustrated in Table 1 below, there are three families of GDRs, distinguished by increasing latency and accuracy, going from the Operational GDR (OGDR), to the Interim GDR (IGDR), to the final GDR. Within each of these three families there are up to three types of files in NetCDF format, with increasing size and complexity:

1. a reduced 1 Hz subset of the full dataset in NetCDF format (O/I/GDR-SSHA);
2. the native NetCDF formatted datasets (O/I/GDRs) which contain 1Hz records as well as 20 Hz high-rate values;
3. an expert sensor product containing the full radar-echo waveforms in NetCDF format (S-IGDR/S-GDR, not applicable to the OGDR).

For the OGDR family, a specific product in BUFR format containing exclusively 1 Hz data is available, designed to cover the needs of the operational community for near real time observations in World Meteorological Organisation (WMO) standardised formats for assimilation in Numerical Weather Prediction (NWP) models.

Jason-3 Level-2 Products

	OGDR Family	IGDR Family	GDR Family	
Reduced 1Hz	OGDR-SSHA	IGDR-SSHA	GDR-SSHA	<div style="text-align: right; color: red; font-weight: bold;">Size & Complexity</div> <div style="display: flex; justify-content: center; align-items: center;"> <div style="border-left: 1px solid black; height: 100px; margin-right: 10px;"></div> <div style="border-left: 1px solid black; height: 100px;"></div> </div>
1Hz + 20Hz	OGDR OGDR-BUFR*	IGDR	GDR	
1Hz + 20Hz + Waveforms		S-IGDR	S-GDR	
Latency:	3-5 Hours	1-2 Days	~ 90 Days	

Latency

Accuracy

* All files in NetCDF format except OGDR-BUFR, which contains no 20-Hz data

Table 2 : Summary of operational, interim, and final geophysical data record products (O/I/GDR) from Jason-3.

All nine files contain sea surface height, ocean surface wind speed, significant wave height information and all required corrections. The NetCDF files differ in the amount and type of auxiliary data included but the product format is the same.

1.1.2. Filename conventions

The product names are based on the following convention:

JA3_<O/I/G>P<N/R/S>_2P<v><S/P><ccc>_<ppp>_<yyyymmdd_hhnss>_<yyyymmdd_hhnss>.nc



With :

<O/I/G> : product family (O : OGDR, I : IGDR, G: GDR)
<N/R/S> : product type (N : native, R: reduced, S : sensor)
<v> : product version (set to 'T' during CalVal phases)
<S/P> : product duration (S : segment for OGDR, P : pass for I/GDR)
<ccc>: cycle number of 1st product record
<ppp> : pass number of 1st product record (1-254)
<yyyymmdd_hhnnss> : date of 1st product record
<yyyymmdd_hhnnss> : date of last product record

So for the OGDR we have:

OGDR: JA3_OPN_2PvSccc_ppp_yyyymmdd_hhnnss_yyyymmdd_hhnnss.nc
OGDR-SSHA: JA3_OPR_2PvSccc_ppp_yyyymmdd_hhnnss_yyyymmdd_hhnnss.nc

For the OGDR-BUFR, the filename is not relevant if you are accessing the files via GTS (see below for details on access to NRT data). Otherwise, if you are accessing the files from the archives (NCEI or UMARF) or EUMETCast, the filenames of the OGDR-BUFR are:

at the NOAA/NCEI:

JA3_OPB_2PvSccc_ppp_yyyymmdd_hhnnss_yyyymmdd_hhnnss

at the EUMETSAT/UMARF and on EUMETCast:

W_US-NOAA-

Washington,SURFACE+SATELLITE,JASON3+OGDR_C_KNES_yyyymmddhhnnss_v_ccc_pp
pp_yyyymmddhhnnss.bin

W_XX-EUMETSAT-

Darmstadt,SURFACE+SATELLITE,JASON3+OGDR_C_EUMS_yyyymmddhhnnss_v_ccc_pp
p_yyyymmddhhnnss.bin

for the IGDR:

IGDR: JA3_IPN_2PvPccc_ppp_yyyymmdd_hhnnss_yyyymmdd_hhnnss.nc
IGDR-SSHA: JA3_IPR_2PvPccc_ppp_yyyymmdd_hhnnss_yyyymmdd_hhnnss.nc
S-IGDR: JA3_IPS_2PvPccc_ppp_yyyymmdd_hhnnss_yyyymmdd_hhnnss.nc

and for the GDR:

GDR: JA3_GPN_2PvPccc_ppp_yyyymmdd_hhnnss_yyyymmdd_hhnnss.nc
GDR-SSHA: JA3_GPR_2PvPccc_ppp_yyyymmdd_hhnnss_yyyymmdd_hhnnss.nc
S-GDR: JA3_GPS_2PvPccc_ppp_yyyymmdd_hhnnss_yyyymmdd_hhnnss.nc



1.2. Handbook Overview

This is a combination of a guide to data use and a reference handbook, so not all sections will be needed by all readers.

Section 1 provides information on product evolution history

Section 2 provides background information about the (O)(I)GDR and this document

Section 3 is an overview of the Jason-3 mission

Section 4 is an introduction to using the Jason-3 data

Section 5 is an introduction to the Jason-3 altimeter algorithms

Section 6 provides a description of the content and format of the Jason-3 (O)(I)GDRs

Appendix A contains references

Appendix B contains acronyms

Appendix C describes how to order information or data from CNES, EUMETSAT and NOAA, and lists related Web sites.

1.3. Document reference and contributors

When referencing this document, please use the following citation:

“Jason-3 Products Handbook”,

CNES :	SALP-MU-M-OP-16118-CN
EUMETSAT :	TBD
JPL :	TBD
NOAA/NESDIS :	TBD

Other contributors include:

J.P. Dumont, L. Carrère, S. Urien, H. Roinard and V. Rosmorduc from CLS

J. Lillibridge from NOAA

S. Desai from NASA/JPL

H. Bonekamp, Remko Scharroo and J. Figa from EUMETSAT

F. Bignalet-Cazalet, E. Bronner, A. Couhert, A. Guillot and N. Picot from CNES

1.4. Conventions

1.4.1. Vocabulary

1.4.1.1. Altimetric distances

In order to reduce confusion in discussing altimeter measurements and corrections, the following terms are used in this document as defined below:

- **Distance** and **Length** are general terms with no special meaning in this document

- **Range** is the distance from the satellite to the surface of the Earth, as measured by the altimeter. Thus, the altimeter measurement is referred to as "range" or "altimeter range," not height
- **Altitude** is the distance of the satellite or altimeter above a reference point. The reference point used is the reference ellipsoid. This distance is computed from the satellite ephemeris data
- **Height** is the distance of the sea surface above the reference ellipsoid. The sea surface height is the difference of the altimeter range from the satellite altitude above the reference ellipsoid

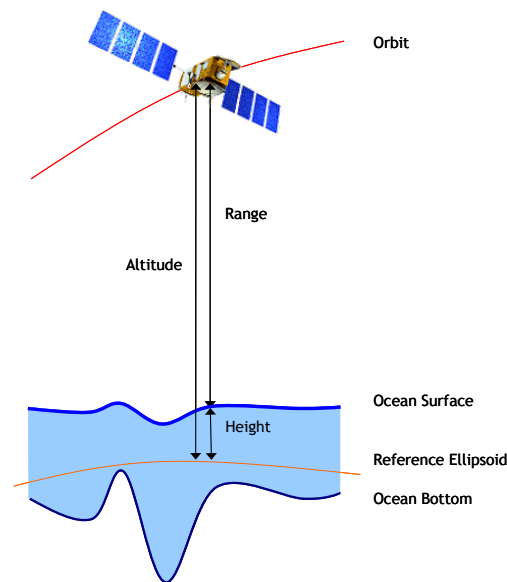


Figure 1 : Altimetric distances - Altitude, Range and Height

1.4.1.2. Orbits, Revolutions, Passes, and Repeat Cycles

An **Orbit** is one circuit of the earth by the satellite as measured from one ascending node crossing to the next. An ascending node occurs when the sub satellite point crosses the earth's equator going from south to north. A **Revolution** (REV) is synonymous with orbit.

The OGDR data is organized into files ("segments") which corresponds to the amount of data dumped over an Earth terminal (typically 2 hour-data sets).

The (I)GDR data is organized into pass files in order to avoid having data boundaries in the middle of the oceans, as would happen if the data were organized by orbit. A **Pass** is half a revolution of the earth by the satellite from extreme latitude to the opposite extreme latitude.

For Jason-3, an **Ascending Pass** begins at the latitude -66.15 deg and ends at +66.15 deg. A **Descending Pass** is the opposite (+66.15 deg to -66.15 deg). The passes are numbered from 1 to 254 representing a full repeat cycle of the Jason-3 ground track. Ascending passes are odd numbered and descending passes are even numbered.

After one **repeat cycle** of 254 passes, Jason-3 revisits the same ground-track within a margin of ± 1 km. That means that every location along the Jason-3 ground-track is measured every approximately 9.9 days.



1.4.1.3. Reference Ellipsoid

For GDR-F Standard, the **Reference Ellipsoid** is the first-order definition of the non-spherical shape of the Earth as an ellipsoid of revolution with equatorial radius of 6378.1370 kilometers and a flattening coefficient of 1/298.257223563 (WGS84 ellipsoid).

1.4.2. Correction Conventions

All environmental and instrument corrections are computed so that they should be added to the quantity which they correct. That is, a correction is applied to a measured value by

$$\text{Corrected Quantity} = \text{Measured Value} + \text{Correction}$$

This means that a correction to the altimeter range for an effect that lengthens the apparent signal path (e.g., wet troposphere correction) is computed as a negative number. Adding this negative number to the uncorrected (measured) range reduces the range from its original value toward the correct value. Example: Corrected Range = Measured Range + Range Correction.

1.4.3. Time Convention

Times are UTC and referenced to **January 1, 2000 00:00:00.00**.

A UTC leap second can occur on June 30 or December 31 of any year. The leap second is a sixty-first second introduced in the last minute of the day. Thus the UTC values (minutes:seconds) appear as: 59:58 ; 59:59 ; 59:60 ; 00:00 ; 00:01.

1.4.4. Unit Convention

All distances and distance corrections are reported in tenths of millimeters (10^{-1} mm).

1.4.5. Flagging and Editing

In general, flagging consists of three parts: instrument flags (on/off), telemetry flags (preliminary flagging and editing) and data quality flags (geophysical processing flags).

Instrument flags provide information about the state of the various instruments on the satellite.

Telemetry flags are first based on instrument modes and checking of telemetry data quality. Only severely corrupted data are not processed (i.e. data that cannot be correctly read on ground). Flag setting is designed to get a maximum amount of data into the "Sensor Data Records" (part of the SGDR data sets). Science data are processed only when the altimeter is in tracking mode.

Quality flags are determined from various statistical checks on the residuals after smoothing or fitting through the data themselves. These flags are set if gaps in the data are detected, or residuals have exceeded predetermined thresholds, or if the gradients of the data exceed predetermined thresholds.



2. Jason-3 Mission Overview

2.1. Background

Three previous high-accuracy altimetric missions, TOPEX/POSEIDON (T/P, launched in August 1992 and which last until October 2005), Jason-1 (launched in December 2001, stopped in June 2013) and Jason-2 (launched in June 2008, stopped in October 2019) have been the key elements of a major turning point in physical oceanography, in terms of both scientific research and applications. Exceeding most initial specifications in terms of accuracy, T/P quickly became a unique tool to make significant progress in the understanding and modeling of ocean circulation and consequently on its climatic impact. The success of the T/P mission was mainly due to an appropriate optimization of the system: instruments, satellite, and orbit parameters were all specifically designed to fulfill the objectives of the mission. The T/P follow-on mission, Jason-1, was engaged soon after with the aim to provide the same level of performance, but with a significant decrease in weight and power needs, hence a much lower mission cost. In addition, near-real time applications were included in the main objectives of the mission. Jason-2 presents better tracking performance and continues the success story of altimetric missions.

These missions, individually as well as combined have made essential contributions in other domains, like mean sea level surveys, tides, marine meteorology, geophysics and geodesy. Most notably the tandem mission phases, where Jason-1 and T/P or Jason-1 and Jason-2 were flying on the same orbit separated by only 70 s or 1 min, provided a unique opportunity for intercalibration of both systems, hence improving further the scientific data quality. High accuracy radar altimeter missions are uniquely capable to globally and continuously observe the ocean and to better understand the short to long term changes of ocean circulation. They are now considered as essential components of global ocean observation systems. These systems integrate altimetric and other satellites and in-situ data into models and require the continuity and permanence of ocean measurements to produce time series over several decades.

The near-real time and short term capability of Jason-1 (decommissioned in July 2013) , Jason-2 as well as ENVISAT (from ESA, launched in March 2002 and decommissioned in June 2012) have fed several pilot experiments that demonstrated the growing importance of operational ocean observation products and short-range ocean prediction for a variety of applications (ship routing, environmental hazards, support to maritime industries).

Also worth mentioning is the importance of wave and wind data provided by altimeter systems over oceans. This information is routinely used in meteorological and research entities, either for calibration of other data sets, assimilation in weather and wave models, or for statistical analysis.

2.2. Introduction to Jason-3 Mission

2.2.1. Mission overview

The Jason-3 mission follows in the footsteps of the TOPEX/POSEIDON, Jason-1 and Jason-2 missions and provides continuity with those missions, with two driving ambitions:

- Ensuring continuity of high quality measurements for ocean science
- Providing operational products for assimilation and forecasting applications

The planned service life of Jason-3 stands at five years (including extended observation phase) after its launch. The mission objective is therefore to provide operational continuity for the collection and distribution of high-precision data for the study of ocean currents and the measurement of sea levels, with a view to improving understanding of these phenomena and their impact on the climate.



The Jason-3 mission takes also into account the feedback from the altimetry series. Thus, the Ocean Surface Topography Science Team, in its annual meeting in Seattle in 2009, has emphasized the need of stability across several mission lifetimes for global mean sea level measurement.

The Jason-3 mission fulfills the role of reference mission for the ocean surface topography constellation, recognized by the Marine Core Service (MyOcean) of GMES called **CMEMS**.

2.2.2. Mission objectives

The importance of altimetry data to better understand the ocean circulation and its impact on the climate of the Earth led to the TOPEX/Poseidon and Jason-1 missions, followed by OSTM/JASON-2 mission with a satellite launched in June 2008. These missions initiated a data collection effort that must continue well into the decades to come in order to monitor the inter-annual evolution and separate transient phenomena from secular variations.

Thus, it is the aim of the follow-on to TOPEX/Poseidon, Jason-1 and OSTM/Jason-2 missions, to provide on a continuous basis, the same high accuracy altimetric measurements designed to study ocean circulation and sea surface elevation.

Since OSTM/Jason-2, the additional objective has been to bring high precision altimetry to a full operational status, through the continued collection of measurements of sea surface height (SSH), significant wave height (SWH), wind speed at the ocean surface and other parameters which was initiated by TOPEX/Poseidon and Jason-1 missions.

OSTM/Jason-2 provides Data Products to the operational and research communities, in support of :

1) Operational Applications such as:

- Marine Meteorology;
- Short Medium-Range and Seasonal Forecasting;

2) Climate Application and Forecasting such as:

- Sea Level Rise and Climate Change;
- Ocean, Earth system and climate research.

The Jason-3 mission will provide Data products to the same user communities, on a continuous basis and with the same required accuracy as Jason-2.

In addition to these objectives other science objectives are covered by passenger experiments. They are aimed at improving the knowledge of the radiation environment at the JASON orbit level.

2.2.3. Mission partnership

The Jason-3 mission was determined as part of an agreement between four partners: CNES, NASA, NOAA and EUMETSAT.

The Jason-3 Programme is led by the operational agencies EUMETSAT and NOAA, with CNES making a significant in-kind contribution and acting at technical level as the system coordinator. NASA in conjunction with EUMETSAT, NOAA and CNES will support science team activities.

NOAA responsibilities are :

- Lead with EUMETSAT the Jason-3 Programme.
- To provide support to the overall system engineering.
- To provide the U.S. payload consisting of an Advanced Microwave Radiometer (AMR) with its antenna, a laser retroreflector array (LRA), and a Global Positioning System Payload (GPSP) receiver package. This point will be conducted by NASA, in coordination with NOAA.
- Provide launch services compatible with the Jason-3 satellite and the mission requirements. This point will be conducted by NASA, in coordination with NOAA.



Jason-3 Products Handbook

Iss :2.1 - date : June 21^h , 2021



9

- Provide and operate a command and control center for the satellite, command and data acquisition stations.
- Provide and operate near real-time data processing for data collected by NOAA ground stations.
- Provide dissemination of all near real-time data products (NOAA and EUMETSAT) and offline data products.
- Provide a long-term archive of all near real-time and offline data products including telemetry, orbital and auxiliary data sets.
- Support the relevant Research Announcement process, and assess the relevance of investigation results for future operational services.

EUMETSAT responsibilities are :

- Lead with NOAA the Jason-3 Programme.
- Provide support to the overall system engineering.
- Fund the European payload consisting of the Poseidon dual-frequency radar altimeter with its antenna, and the Doppler Orbitography and Radiopositioning Integrated by Satellite (DORIS) receiver package, the payload module and its integration. This payload development will be conducted by CNES, in coordination with EUMETSAT.
- Provide and operate near real-time data processing for data collected by European ground station(s).
- Provide dissemination of all near real-time data products (NOAA and EUMETSAT).
- Fund a command and control center for the satellite, a European Earth Terminal and the offline data processing, archiving and dissemination for the Programme. The development of these elements will be conducted by CNES, in coordination with EUMETSAT.
- Support the relevant Research Announcement process, and assess the relevance of investigation results for future operational services.

CNES responsibilities are :

- Provide as in-kind contribution :
 - system engineering and associated human resources
 - standard flightworthy PROTEUS platform
 - CNES human resources as part of the operations.
- On behalf of EUMETSAT, procure the Jason-3 satellite including the European payload (Poseidon dual-frequency radar altimeter with its antenna, and the Doppler Orbitography and Radiopositioning Integrated by Satellite (DORIS) receiver package) , the payload module, the command and control center for the satellite, a European Earth Terminal both near-real time and offline data processing, archiving and dissemination for the mission.
- Conduct and coordinate with the partners the preparation and release of relevant Research Announcements.
- Conduct, in coordination with EUMETSAT, the selection of European Investigators.

NASA responsibilities are :

- Conduct and coordinate with the partners the preparation and release of relevant Research Announcements.
- Conduct, in coordination with NOAA the selection of U.S. Investigators.



And finally, NOAA, EUMETSAT, NASA and CNES have the joint responsibility to establish and jointly operate a Jason-3 Ground Segment. Telemetry would be made available to the partners and data products would be made available to the broader international user community through data centers under the responsibilities of the partners consistent with the provisions on data policy in the MOU.

Data Products which commit the Operational Agencies (EUMETSAT and NOAA) will be, at a minimum, consistent with TOPEX/Poseidon, Jason-1 and Jason-2 data products, in line with the global data requirements for satellite altimetry missions (AD5). They will be defined in the Mission Requirements Document (AD3) and detailed in the Operational Service Specification (OSS) (AD2) together with the associated services to the users.

As on OSTM/Jason-2 mission, the availability of a continued data stream from altimetric measurements with near real-time access will result in the participation in this mission of NOAA and EUMETSAT agencies interested in the operational applications of these data.

Jason-3 operations are planned for five years.

2.2.4. Mission launch

Jason-3 was launched on January 17th, 2016 at 18H42 (UTC) from the Vandenberg Air Force Base (California) by a Falcon 9 vehicle (Space X Company) and reached its nominal repetitive orbit on February 12th, 2016. The start of cycle 1 occurred on February 17th at 10:28:45 (UTC).

2.3. Jason-3 Requirements

The major elements of the mission include:

- **An Earth orbiting satellite carrying an altimetric system** for measuring the height of the satellite above the sea surface
- **A precision orbit determination system** for referring the altimetric measurements to geodetic coordinates
- **A data analysis and distribution system** for processing the satellite data, verifying their accuracy, and making them available to the scientific community
- **A Principal Investigator program** for feedback from operational applications and scientific studies based on the satellite observations

The sea-surface height measurement must be made with an accuracy of 3.4 cm or better (at 1 Hz) in order to meet the mission objectives. The Jason-3 satellite is specified and designed to fulfill the mission objectives (AD 1) and to take over from the Jason-1/2 missions. As for Jason-1/2, distribution of altimetric products (non-validated) in near real time is planned. The interim (IGDR) and definitive (GDR) science products are delivered later (see Table 20 in section 6), following the model used for Jason-1 and Jason-2.

To ensure that science and mission goals are accomplished by the Jason-3 mission, the following requirements were established.

2.3.1. Accuracy of Sea-level Measurements

Generally speaking Jason-3 has been specified based on the Jason-2 state of the art, with no major change on ground segment but some changes in the instrumentation (mostly in GPS and DORIS). We can only mention the following differences: on-board automatic transitions between the Diode/DEM (Digital Earth Model) mode and the acquisition/tracking mode depending on the satellite's position, information about altimeter mode in the telemetry and differences about radiometer calibrations. As for Jason-2 the sea-surface height shall be provided with a globally averaged RMS accuracy of 3.4 cm (1 sigma), or better, assuming 1 second averages.



The instrumental and environmental corrections are provided with the appropriate accuracy to meet this requirement. In addition to these requirements, a set of measurement-system goals was established based on the anticipated impact of off-line ground processing improvements. These improvements are expected to enable reduction of sea-surface height errors to 2.5 cm RMS. Knowledge of the stability of the system is especially important to the goal of monitoring the change in the global mean sea level, hence a specification on the system drift with a 1 mm/year goal.

The following table provides a summary of specifications and error budget at the end of the verification phase of Jason-2.

Parameter	OGDR 3 hours		IGDR 1 to 1.5 days		GDR 40 days		
	Requirement	Actual	Requirement	Actual	Requirement	Goal	Actual
Altimeter Noise ¹	1.7	1.8	1.7	1.8	1.7	1.5	1.8
Ionosphere ²	1	0.3	0.5	0.3	0.5	0.5	0.3
Sea State Bias ³	3.5	2	2	2	2	1	2
Dry Troposphere	1	0.8	0.7	0.7	0.7	0.7	0.7
Wet Troposphere	1.2	0.8	1.2	0.8	1.2	1	0.8
Altimeter Range, RSS	5	2.9	3	2.9	3	2.25	2.9
RMS Orbit (Radial Component)	10 ⁽⁴⁾	3.0 ⁽⁴⁾	2.5	1.5	1.5	1.0	1.0
Total Sea Surface Height, RSS	11.2	4.2	3.9	3.3	3.4	2.5	3.1
Significant Wave Height ⁵	10% or 0.5 m	TBD % or 0.12 m	10% or 0.4m	TBD % or 0.12 m	10% or 0.4m	5% or 0.25m	TBD % or 0.12 m
Wind Speed	1.6 m/s	0.9 m/s	1.5 m/s	0.9 m/s	1.5 m/s	1.5 m/s	0.9 m/s
Sigma Naught (absolute)	0.7 dB	0.1 ⁽⁶⁾ dB	0.7 dB	0.1 ⁽⁶⁾ dB	0.7 dB	0.5 dB	0.1 ⁽⁶⁾ dB
System Drift						1 mm/year ⁽⁷⁾	TBD

(1) – Ku-Band after ground retracking, averaged over 1 second, assuming 320 MHz C-Band bandwidth.
(2) – Filtered over 100 km assuming 320 MHz bandwidth.
(3) – Can also be expressed as 1% of SWH.
(4) – Real-time DORIS onboard ephemeris.
(5) – Whichever is greater.
(6) – After calibration to Jason-1.
(7) – On global mean sea level, after calibration.

Table 3 : Summary of error budget at the end of the verification phase of Jason-2

2.3.2. Sampling Strategy

As for Jason-2, sea level shall be measured along a fixed grid of sub satellite tracks such that it is possible to investigate and minimize the spatial and temporal aliases of surface geostrophic currents and to minimize the influence of the geoid on measurements of the time-varying topography.

2.3.3. Tidal Aliases

As for Jason-2, sea level shall be measured such that tidal signals are not aliased into semiannual, annual, or zero frequencies (which influences the calculation of the permanent circulation) or frequencies close to these.

2.3.4. Duration and coverage

Sea level shall be measured for a minimum of five years, with the potential to extend this period for an additional two years.

The Jason-3 satellite shall overfly the reference Jason-2 ground tracks.



2.4. Satellite Description

The 500 kg satellite consists of a multi-mission PROTEUS platform and a Jason-3 specific payload module. The platform provides all housekeeping functions including propulsion, electrical power, command and data handling, telecommunications, and attitude control. It is provided by CNES. The payload module provides mechanical, electrical, thermal, and dynamical support to the Jason-3 instruments.

The Jason-3 payload (see Figure 2) includes the following components:

- **An Altimeter (Poseidon-3B)**, provided by CNES - the main mission instrument
- **A Microwave Radiometer (AMR)**, provided by NASA - to correct the altimeter measurement for atmospheric range delays induced by water vapor
- **The radio positioning DORIS system**, provided by CNES - for precision orbit determination using dedicated ground stations
- **A Laser Reflector Array**, provided by NASA - to calibrate the orbit determination system
- **A precision GPS receiver (GPSP)**, provided by NASA - to provide supplementary positioning data to DORIS in support of the POD function and to enhance and/or improve gravity field models
- Two experimental passengers:
 - **CARMEN-3 Radiation Detectors**, provided by CNES - to measure high-energy particles that could disturb the ultra-stable oscillator in the DORIS positioning unit
 - **A Light Particle Telescope (LPT) detection unit**, provided by JAXA under CNES responsibility - complementing the measurement of radiation received by the DORIS instrument

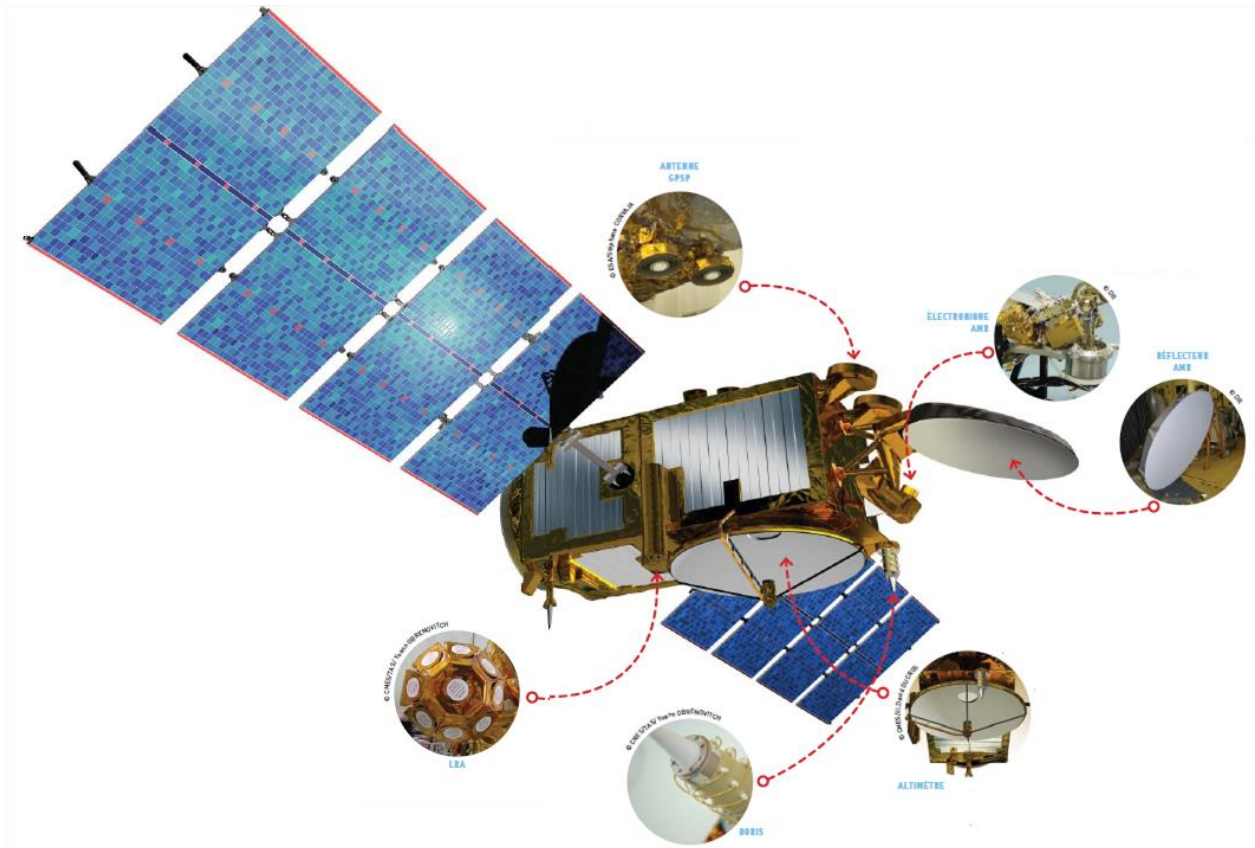


Figure 2 : Main components of the Jason-3 satellite

2.4.1. Satellite Characteristics

The main features of the Jason-3 satellite are summed up in the following table.

Satellite mass	510 kg
Satellite power	703 W
Platform mass	264 kg
Platform power	239 W
Payload mass	119 kg
Payload power	236 W
Altimeter mass	46 kg
Altimeter power	84 W
Launch Vehicle	Falcon 9
Launch Site	Vandenberg Air Force Base (California)

Table 4 : Main features of the Jason-3 satellite

2.4.2. Sensors

2.4.2.1. Poseidon-3B Altimeter

The two-frequency solid-state altimeter, measuring range with accurate ionospheric corrections, is derived from the two-frequency Poseidon-3 altimeter embarked on Jason-2 mission. It operates at 13.575 GHz (Ku-band) and 5.3 GHz (C-band). Poseidon-3B electronics are configured in two boxes: the processing unit (PCU) and the radiofrequency unit (RFU).

- The processing unit includes the digital chirp generator, base-band demodulator, spectrum analyzer, instrument control unit and interfaces.
- The RF unit includes the up-conversion to the Ku and C bands, high power amplifier (solid state), low noise amplification of the received echoes and mixing with a reference chirp. The peak output powers are 6 to 8 W for the Ku band and 25 W for the C band.
- Poseidon-3B is dual string (in cold redundancy) without cross strapping and connected to the antenna through a switching box.
- Poseidon-3B antenna is of centered type (1.2 meter diameter) and located on the nadir face of the satellite.



Figure 3 : Jason-3 Poseidon-3 Instrument

2.4.2.2. Advanced Microwave Radiometer (AMR)

The three frequency microwave radiometer, named the Advanced Microwave Radiometer, consists of three separate channels at 18.7, 23.8 and 34 GHz. The radiometer is equivalent to the Advanced



Microwave Radiometer found on Jason-2. The 23.8 GHz channel is the primary water vapor sensing channel, meaning higher water vapor concentrations leads to larger 23.8 GHz brightness temperature values. Moreover, the 34 GHz channel and the 18.7 GHz channel, which have less sensitivity to water vapor, facilitate the removal of the contributions from cloud liquid water and excess surface emissivity of the ocean surface due to wind, which also act to increase the 23.8 GHz brightness temperature.

The AMR design is based on Monolithic Millimeter-wave Integrated Circuit (MMIC) technology and represents a giant leap forward from its predecessors (TMR and JMR) in both mass and size. Three redundant temperature controlled noise diodes are used for operational gain calibration in all the radiometers channels. The use of noise diodes eliminates the need for a cold sky calibration horn, which was employed on TMR. The JMR was the first space-borne radiometer to use noise diodes for calibration and the AMR is the second.

Another significant improvement in the AMR design is the addition of a 1-m reflector, compared to a 0.6 m reflector for TMR and JMR, which nearly doubles the spatial resolution of the AMR. The AMR is expected to produce reliable path delay measurements to within 15-20 km from the coast. The antenna is a fixed offset paraboloid (1 meter diameter) fed by a single three frequency coaxial corrugated horn feed. It is located on the front of the satellite (+ X axis) and its beam is co-aligned with the altimeter footprint.

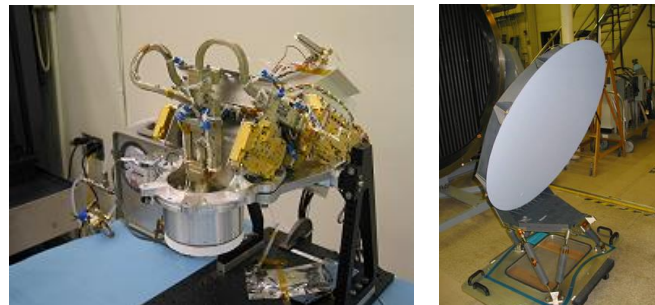


Figure 4 : Jason-3 AMR Instrument and Antenna

2.4.2.3. DORIS System

The complete DORIS system includes the DORIS on board package, a network of approximately 50 beacons located around the world and a ground system.

The on board package includes the receiver itself, the ultrastable oscillator and an omnidirectional antenna located on the nadir face of the satellite.

The DORIS on board package is a new version of the DORIS instrument (all the functions included in a single unit). It includes a 8-beacons receiving capability and an on-board real time function (DIODE = “*Détermination Immédiate d’Orbite par DORIS Embarqué*”) to compute the orbit ephemeris.

The DORIS on board package is also dual string (in cold redundancy) without cross strapping and connected to the single antenna through a switching box. Each receiver is connected to its own ultra stable oscillator.

The DORIS antenna is located on the nadir side of the satellite.



Figure 5 : Jason-3 DORIS Receiver Antenna and Instrument

2.4.2.4. Laser Reflector Array

The laser reflector array is placed on the nadir face of the satellite. It consists of several quartz corner cubes arrayed as a truncated cone with one in the center and the others distributed azimuthally around the cone.

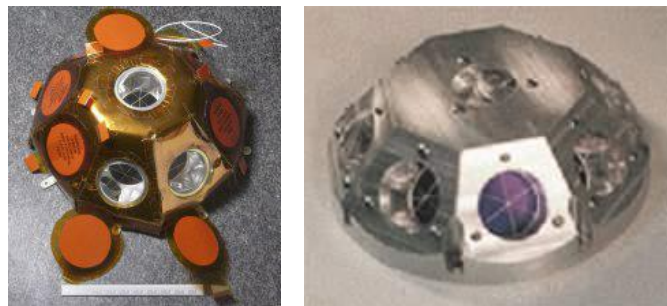


Figure 6 : Jason-3 Laser Reflector Array

2.4.2.5. GPS Receiver

The GPS Payload receiver is a twelve channel Global Positioning system receiver. The on board package is comprised of a down-converter processor assembly, two antennas and interconnecting RF cables.

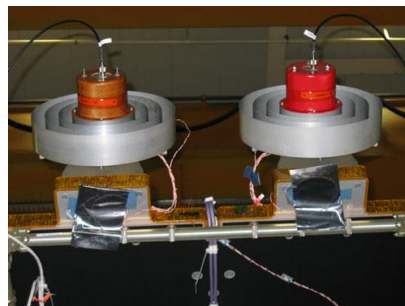


Figure 7 : Jason-3 Precision GPS Receiver

2.4.2.6. CARMEN-3 Radiation Detectors

CARMEN-3 is the mission name for the ICARE-NG instrument aboard Jason-3 satellite.

This instrument is dedicated to study the influence of space radiation on advanced components to measure e⁻, p⁺ and ion fluxes in the energy ranges responsible for component effects (as ionizing dose, single event effect and displacement damage), to measure associated effects on test components, to characterize the local radiation environment for DORIS USO and to evaluate its potential drifts inside the SAA.

The on board package includes only ICARE-NG box that is composed of a CPU, data processing & TM/TC unit, a custom DC/DC converter, a Data acquisition unit for the set of three radiation detectors and the component test bed.



Figure 8 : Jason-3 CARMEN-3 Instrument

2.4.2.7. LPT Detection Unit

The LPT Detection Unit is composed of one detector box (LPT) and one electronic box (LPT-E). All the electrical interfaces with the satellite are through the LPT-E.

The detectors are placed on the satellite in order to see the same radiation environment and at the vicinity of DORIS BDR. The LPT-S is an assembly of four sensors, each adapted to different particles and energy band.



Figure 9 : Jason-3 LPT

2.4.3. Orbit

2.4.3.1. Repetitive orbit on historical ground track (January 2016 - April 2022)

The Jason-3 satellite flies on the same ground-track as the original Jason-2, the original Jason-1 and the original T/P with a 254 pass, 10-day exact repeat cycle. During the Jason-3 Cal/Val phase, Jason-3 was placed close to Jason-2 (1 minute 20 s apart) in order to allow inter-calibration of all systems. Then Jason-2 was moved to an interleaved ground track in October 2016 (as was Jason-1 in January 2009).

Orbital characteristics and the equator crossing longitudes for Jason-3 are given in Tables 10 and 11.

Figure below is a plot of the ground track on a world map.

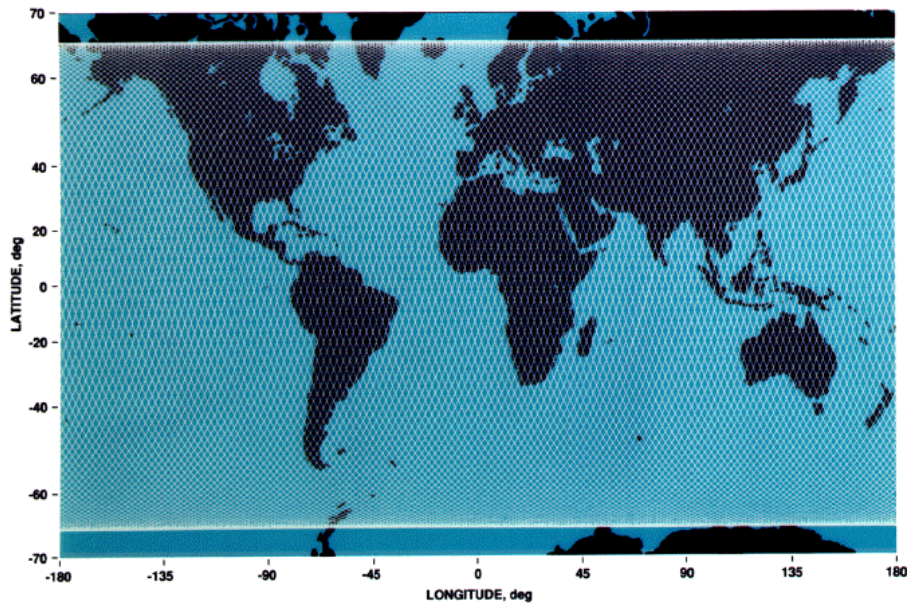


Figure 10 : T/P, Jason-1 (reference orbit), OSTM/Jason-2 and Jason-3 ground track coverage every 10 days

→ The mean classical orbit elements are given in the table below.

Orbit element	Value
Semi-major axis	7,714.432 km
Eccentricity	0.000098
Inclination	66.042 deg
Argument of periapsis	90.0 deg

Table 5 : Mean classical orbit elements

→ The orbit auxiliary data are given in the table below.

Auxiliary Data	Values
Mean equatorial altitude over 1 cycle (WGS84 ellipsoid)	1339.65 Km
Nodal period	6,745.7605 sec
Repeat period	9.91564 days
Number of revolutions within a cycle	127
Equatorial cross-track separation	315.55 km
Ground track control band	± 1 km (at equator)
Acute angle at Equator crossings	39.4 deg
Longitude of Equator crossing of pass 1	99.9242 deg
Inertial nodal rate	-2.07707 deg/day
Orbital speed	7.2 km/s
Ground track speed	5.8 km/s

Table 6 : Orbit auxiliary data

This orbit overflies two verification sites funded by NASA and CNES. The prime CNES verification site is located at Cape Senetosa on the island of Corsica (8°48' E, 41°34' N, ascending pass 85). The



Jason-3 Products Handbook

Iss :2.1 - date : June 21^h , 2021



19

prime NASA verification site is located on the Harvest oil platform near Pt. Conception, California (239° 19' E, 34° 28' N, ascending pass 43).

A satellite orbit slowly decays due to air drag, and has long-period variability because of the inhomogeneous gravity field of Earth, solar radiation pressure, and smaller forces. Periodic maneuvers are required to keep the satellite in its orbit. The frequency of maneuvers depends primarily on the solar flux as it affects the Earth's atmosphere, and there are expected to be one maneuver (or series of maneuvers) every 40 to 200 days.

Each orbit maintenance maneuver is performed using only one thrust to minimize impacts on the ground orbit solution. Orbit computation is optimized to minimize the orbit error during such periods. Science data are taken during orbit maintenance maneuvers and are distributed (an orbit state flag is provided in the products).



2.4.3.1.1. Equator Crossing Longitudes (in order of Pass Number)

Pass	Longitude	Pass	Longitude	Pass	Longitude	Pass	Longitude	Pass	Longitude	Pass	Longitude
1	99.9249	44	30.4744	87	321.0274	130	251.5783	173	182.1282	216	112.6813
2	265.7517	45	196.3012	88	126.8541	131	57.4042	174	347.9550	217	278.5075
3	71.5776	46	2.1280	89	292.6810	132	223.2310	175	153.7829	218	84.3343
4	237.4044	47	167.9557	90	98.5078	133	29.0576	176	319.6096	219	250.1600
5	43.2305	48	333.7825	91	264.3336	134	194.8843	177	125.4369	220	55.9867
6	209.0573	49	139.6102	92	70.1603	135	0.7117	178	291.2636	221	221.8129
7	14.8844	50	305.4370	93	235.9862	136	166.5385	179	97.0902	222	27.6397
8	180.7112	51	111.2637	94	41.8130	137	332.3659	180	262.9170	223	193.4666
9	346.5387	52	277.0905	95	207.6395	138	138.1927	181	68.7430	224	359.2934
10	152.3655	53	82.9167	96	13.4663	139	304.0198	182	234.5697	225	165.1212
11	318.1928	54	248.7435	97	179.2937	140	109.8466	183	40.3959	226	330.9479
12	124.0196	55	54.5694	98	345.1205	141	275.6727	184	206.2227	227	136.7755
13	289.8463	56	220.3962	99	150.9484	142	81.4995	185	12.0499	228	302.6023
14	95.6731	57	26.2229	100	316.7751	143	247.3252	186	177.8767	229	108.4290
15	261.4989	58	192.0497	101	122.6022	144	53.1520	187	343.7042	230	274.2558
16	67.3256	59	357.8771	102	288.4290	145	218.9782	188	149.5309	231	80.0819
17	233.1515	60	163.7039	103	94.2556	146	24.8050	189	315.3582	232	245.9087
18	38.9783	61	329.5313	104	260.0823	147	190.6320	190	121.1850	233	51.7347
19	204.8049	62	135.3580	105	65.9083	148	356.4588	191	287.0117	234	217.5614
20	10.6317	63	301.1851	106	231.7351	149	162.2866	192	92.8384	235	23.3883
21	176.4592	64	107.0119	107	37.5614	150	328.1133	193	258.6642	236	189.2150
22	342.2860	65	272.8379	108	203.3881	151	133.9409	194	64.4909	237	355.0425
23	148.1139	66	78.6647	109	9.2154	152	299.7676	195	230.3169	238	160.8693
24	313.9406	67	244.4904	110	175.0422	153	105.5943	196	36.1437	239	326.6966
25	119.7676	68	50.3172	111	340.8697	154	271.4211	197	201.9704	240	132.5234
26	285.5944	69	216.1435	112	146.6964	155	77.2471	198	7.7971	241	298.3504
27	91.4209	70	21.9702	113	312.5237	156	243.0739	199	173.6248	242	104.1772
28	257.2477	71	187.7974	114	118.3505	157	48.8999	200	339.4515	243	270.0031
29	63.0736	72	353.6242	115	284.1770	158	214.7267	201	145.2793	244	75.8299
30	228.9004	73	159.4520	116	90.0038	159	20.5536	202	311.1061	245	241.6556
31	34.7268	74	325.2788	117	255.8295	160	186.3804	203	116.9330	246	47.4824
32	200.5535	75	131.1062	118	61.6562	161	352.2079	204	282.7598	247	213.3088
33	6.3809	76	296.9330	119	227.4823	162	158.0346	205	88.5862	248	19.1355
34	172.2076	77	102.7596	120	33.3090	163	323.8620	206	254.4130	249	184.9628
35	338.0351	78	268.5864	121	199.1358	164	129.6887	207	60.2389	250	350.7896
36	143.8619	79	74.4124	122	4.9626	165	295.5157	208	226.0657	251	156.6174
37	309.6891	80	240.2392	123	170.7903	166	101.3425	209	31.8922	252	322.4442
38	115.5159	81	46.0652	124	336.6170	167	267.1683	210	197.7189	253	128.2715
39	281.3423	82	211.8920	125	142.4448	168	72.9951	211	3.5463	254	294.0983
40	87.1690	83	17.7190	126	308.2716	169	238.8209	212	169.3731		
41	252.9947	84	183.5458	127	114.0984	170	44.6477	213	335.2005		
42	58.8215	85	349.3733	128	279.9252	171	210.4741	214	141.0273		
43	224.6476	86	155.2000	129	85.7515	172	16.3009	215	306.8545		



Table 7 : Equator Crossing Longitudes (in order of Pass Number)

2.4.3.1.2. Equator Crossing Longitudes (in order of Longitude)

Pass	Longitude	Pass	Longitude	Pass	Longitude	Pass	Longitude	Pass	Longitude	Pass	Longitude
135	0.7117	118	61.6562	101	122.6022	84	183.5458	67	244.4904	50	305.4370
46	2.1280	29	63.0736	12	124.0196	249	184.9628	232	245.9087	215	306.8545
211	3.5463	194	64.4909	177	125.4369	160	186.3804	143	247.3252	126	308.2716
122	4.9626	105	65.9083	88	126.8541	71	187.7974	54	248.7435	37	309.6891
33	6.3809	16	67.3256	253	128.2715	236	189.2150	219	250.1600	202	311.1061
198	7.7971	181	68.7430	164	129.6887	147	190.6320	130	251.5783	113	312.5237
109	9.2154	92	70.1603	75	131.1062	58	192.0497	41	252.9947	24	313.9406
20	10.6317	3	71.5776	240	132.5234	223	193.4666	206	254.4130	189	315.3582
185	12.0499	168	72.9951	151	133.9409	134	194.8843	117	255.8295	100	316.7751
96	13.4663	79	74.4124	62	135.3580	45	196.3012	28	257.2477	11	318.1928
7	14.8844	244	75.8299	227	136.7755	210	197.7189	193	258.6642	176	319.6096
172	16.3009	155	77.2471	138	138.1927	121	199.1358	104	260.0823	87	321.0274
83	17.7190	66	78.6647	49	139.6102	32	200.5535	15	261.4989	252	322.4442
248	19.1355	231	80.0819	214	141.0273	197	201.9704	180	262.9170	163	323.8620
159	20.5536	142	81.4995	125	142.4448	108	203.3881	91	264.3336	74	325.2788
70	21.9702	53	82.9167	36	143.8619	19	204.8049	2	265.7517	239	326.6966
235	23.3883	218	84.3343	201	145.2793	184	206.2227	167	267.1683	150	328.1133
146	24.8050	129	85.7515	112	146.6964	95	207.6395	78	268.5864	61	329.5313
57	26.2229	40	87.1690	23	148.1139	6	209.0573	243	270.0031	226	330.9479
222	27.6397	205	88.5862	188	149.5309	171	210.4741	154	271.4211	137	332.3659
133	29.0576	116	90.0038	99	150.9484	82	211.8920	65	272.8379	48	333.7825
44	30.4744	27	91.4209	10	152.3655	247	213.3088	230	274.2558	213	335.2005
209	31.8922	192	92.8384	175	153.7829	158	214.7267	141	275.6727	124	336.6170
120	33.3090	103	94.2556	86	155.2000	69	216.1435	52	277.0905	35	338.0351
31	34.7268	14	95.6731	251	156.6174	234	217.5614	217	278.5075	200	339.4515
196	36.1437	179	97.0902	162	158.0346	145	218.9782	128	279.9252	111	340.8697
107	37.5614	90	98.5078	73	159.4520	56	220.3962	39	281.3423	22	342.2860
18	38.9783	1	99.9249	238	160.8693	221	221.8129	204	282.7598	187	343.7042
183	40.3959	166	101.3425	149	162.2866	132	223.2310	115	284.1770	98	345.1205
94	41.8130	77	102.7596	60	163.7039	43	224.6476	26	285.5944	9	346.5387
5	43.2305	242	104.1772	225	165.1212	208	226.0657	191	287.0117	174	347.9550
170	44.6477	153	105.5943	136	166.5385	119	227.4823	102	288.4290	85	349.3733
81	46.0652	64	107.0119	47	167.9557	30	228.9004	13	289.8463	250	350.7896
246	47.4824	229	108.4290	212	169.3731	195	230.3196	178	291.2636	161	352.2079
157	48.9999	140	109.8466	123	170.7903	106	231.7351	89	292.6810	72	353.6242
68	50.3172	51	111.2637	34	172.2076	17	233.1515	254	294.0983	237	355.0425
233	51.7347	216	112.6813	199	173.6248	182	234.5697	165	295.5157	148	356.4588
144	53.1520	127	114.0984	110	175.0422	93	235.9862	76	296.9330	59	357.8771
55	54.5694	38	115.5159	21	176.4592	4	237.4044	241	298.3504	224	359.2934
220	55.9867	203	116.9330	186	177.8767	169	238.8209	152	299.7676		
131	57.4042	114	118.3505	97	179.2937	80	240.2392	63	301.1851		
42	58.8215	25	119.7676	8	180.7112	245	241.6556	228	302.6023		



207	60.2389	190	121.1850	173	182.1282	156	243.0739	139	304.0198
-----	---------	-----	----------	-----	----------	-----	----------	-----	----------

Table 8 : Equator Crossing Longitudes (in order of Longitude)

2.4.3.2. Repetitive orbit on interleaved orbit (April 2022-nowadays)

After approval by the Joint Steering Group (held on 25 Oct. 2021) and recommendation from the 2022 OSTST meeting, the Jason-3 satellite was moved to a new ground track early April 2022 after the end of repeat cycle 226, after more than 7 years of service on the nominal ground track.

The satellite was moved to the same interleaved orbit that was used by Topex from 2002-2005, Jason-1 from 2009-2012, and Jason-2 from October 2016 to July 2017. Several maneuvers were performed between April 7th, 2022, and April 25th, 2022.

Regarding the interleaved Jason-3 orbit.

- Jason-3 uses the same pass numbering scheme adopted by Topex, Jason-1 and OSTM/Jason2 in the interleaved ground track. However, the start time of the Jason-3 and Sentinel-6MF repeat cycles differs by approximately 5 days.
- The first Jason-3 repeat cycle on the new interleaved ground track is cycle 300.
- The Jason-3 altimeter was placed in wait mode and data production (OGDR, IGDR and GDR) was stopped during the transit to the interleaved orbit. It was restarted during cycle 300 with the same requirements for data latency and quality.

2.4.3.2.1. Equator Crossing Longitudes (in order of Pass Number)

Pass	Longitude	Pass	Longitude	Pass	Longitude	Pass	Longitude	Pass	Longitude	Pass	Longitude
1	98.51	44	29.06	87	319.62	130	250.17	173	180.72	216	111.27
2	264.34	45	194.89	88	125.44	131	55.99	174	346.55	217	277.10
3	70.17	46	0.72	89	291.27	132	221.82	175	152.37	218	82.92
4	235.99	47	166.54	90	97.10	133	27.65	176	318.20	219	248.75
5	41.82	48	332.37	91	262.92	134	193.48	177	124.03	220	54.58
6	207.65	49	138.20	92	68.75	135	359.30	178	289.85	221	220.40
7	13.47	50	304.03	93	234.57	136	165.13	179	95.68	222	26.23
8	179.30	51	109.85	94	40.40	137	330.95	180	261.51	223	192.06
9	345.13	52	275.68	95	206.23	138	136.78	181	67.33	224	357.89
10	150.96	53	81.51	96	12.06	139	302.61	182	233.16	225	163.71
11	316.78	54	247.33	97	177.88	140	108.44	183	38.99	226	329.54
12	122.61	55	53.16	98	343.71	141	274.26	184	204.81	227	135.36
13	288.43	56	218.99	99	149.54	142	80.09	185	10.64	228	301.19
14	94.26	57	24.81	100	315.37	143	245.91	186	176.47	229	107.02
15	260.09	58	190.64	101	121.19	144	51.74	187	342.29	230	272.85
16	65.92	59	356.47	102	287.02	145	217.57	188	148.12	231	78.67
17	231.74	60	162.29	103	92.84	146	23.40	189	313.95	232	244.50
18	37.57	61	328.12	104	258.67	147	189.22	190	119.78	233	50.32
19	203.39	62	133.95	105	64.50	148	355.05	191	285.60	234	216.15
20	9.22	63	299.77	106	230.33	149	160.88	192	91.43	235	21.98
21	175.05	64	105.60	107	36.15	150	326.71	193	257.25	236	187.81
22	340.88	65	271.43	108	201.98	151	132.53	194	63.08	237	353.63
23	146.70	66	77.25	109	7.80	152	298.36	195	228.91	238	159.46
24	312.53	67	243.08	110	173.63	153	104.18	196	34.73	239	325.29



25	118.36	68	48.91	111	339.46	154	270.01	197	200.56	240	131.11
26	284.18	69	214.73	112	145.29	155	75.84	198	6.39	241	296.94
27	90.01	70	20.56	113	311.11	156	241.66	199	172.21	242	102.77
28	255.84	71	186.39	114	116.94	157	47.49	200	338.04	243	268.59
29	61.66	72	352.22	115	282.77	158	213.32	201	143.87	244	74.42
30	227.49	73	158.04	116	88.59	159	19.14	202	309.70	245	240.24
31	33.32	74	323.87	117	254.42	160	184.97	203	115.52	246	46.07
32	199.14	75	129.69	118	60.25	161	350.80	204	281.35	247	211.90
33	4.97	76	295.52	119	226.07	162	156.63	205	87.18	248	17.73
34	170.80	77	101.35	120	31.90	163	322.45	206	253.00	249	183.55
35	336.62	78	267.18	121	197.72	164	128.28	207	58.83	250	349.38
36	142.45	79	73.00	122	3.55	165	294.10	208	224.66	251	155.21
37	308.28	80	238.83	123	169.38	166	99.93	209	30.48	252	321.04
38	114.11	81	44.65	124	335.21	167	265.76	210	196.31	253	126.86
39	279.93	82	210.48	125	141.03	168	71.59	211	2.14	254	292.69
40	85.76	83	16.31	126	306.86	169	237.41	212	167.96		
41	251.58	84	182.14	127	112.69	170	43.24	213	333.79		
42	57.41	85	347.96	128	278.52	171	209.06	214	139.62		
43	223.24	86	153.79	129	84.34	172	14.89	215	305.44		

Table 9 : Equator Crossing Longitudes (in order of Pass Number)

2.4.3.2.2. Equator Crossing Longitudes (in order of Longitude)

Pass	Longitude	Pass	Longitude	Pass	Longitude	Pass	Longitude	Pass	Longitude	Pass	Longitude
46	0.72	29	61.66	12	122.61	249	183.55	232	244.50	215	305.44
211	2.14	194	63.08	177	124.03	160	184.97	143	245.91	126	306.86
122	3.55	105	64.50	88	125.44	71	186.39	54	247.33	37	308.28
33	4.97	16	65.92	253	126.86	236	187.81	219	248.75	202	309.70
198	6.39	181	67.33	164	128.28	147	189.22	130	250.17	113	311.11
109	7.80	92	68.75	75	129.69	58	190.64	41	251.58	24	312.53
20	9.22	3	70.17	240	131.11	223	192.06	206	253.00	189	313.95
185	10.64	168	71.59	151	132.53	134	193.48	117	254.42	100	315.37
96	12.06	79	73.00	62	133.95	45	194.89	28	255.84	11	316.78
7	13.47	244	74.42	227	135.36	210	196.31	193	257.25	176	318.20
172	14.89	155	75.84	138	136.78	121	197.72	104	258.67	87	319.62
83	16.31	66	77.25	49	138.20	32	199.14	15	260.09	252	321.04
248	17.73	231	78.67	214	139.62	197	200.56	180	261.51	163	322.45
159	19.14	142	80.09	125	141.03	108	201.98	91	262.92	74	323.87
70	20.56	53	81.51	36	142.45	19	203.39	2	264.34	239	325.29
235	21.98	218	82.92	201	143.87	184	204.81	167	265.76	150	326.71
146	23.40	129	84.34	112	145.29	95	206.23	78	267.18	61	328.12
57	24.81	40	85.76	23	146.70	6	207.65	243	268.59	226	329.54
222	26.23	205	87.18	188	148.12	171	209.06	154	270.01	137	330.95
133	27.65	116	88.59	99	149.54	82	210.48	65	271.43	48	332.37
44	29.06	27	90.01	10	150.96	247	211.90	230	272.85	213	333.79
209	30.48	192	91.43	175	152.37	158	213.32	141	274.26	124	335.21



120	31.90	103	92.84	86	153.79	69	214.73	52	275.68	35	336.62
31	33.32	14	94.26	251	155.21	234	216.15	217	277.10	200	338.04
196	34.73	179	95.68	162	156.63	145	217.57	128	278.52	111	339.46
107	36.15	90	97.10	73	158.04	56	218.99	39	279.93	22	340.88
18	37.57	1	98.51	238	159.46	221	220.40	204	281.35	187	342.29
183	38.99	166	99.93	149	160.88	132	221.82	115	282.77	98	343.71
94	40.40	77	101.35	60	162.29	43	223.24	26	284.18	9	345.13
5	41.82	242	102.77	225	163.71	208	224.66	191	285.60	174	346.55
170	43.24	153	104.18	136	165.13	119	226.07	102	287.02	85	347.96
81	44.65	64	105.60	47	166.54	30	227.49	13	288.43	250	349.38
246	46.07	229	107.02	212	167.96	195	228.91	178	289.85	161	350.80
157	47.49	140	108.44	123	169.38	106	230.33	89	291.27	72	352.22
68	48.91	51	109.85	34	170.80	17	231.74	254	292.69	237	353.63
233	50.32	216	111.27	199	172.21	182	233.16	165	294.10	148	355.05
144	51.74	127	112.69	110	173.63	93	234.57	76	295.52	59	356.47
55	53.16	38	114.11	21	175.05	4	235.99	241	296.94	224	357.89
220	54.58	203	115.52	186	176.47	169	237.41	152	298.36	135	359.30
131	55.99	114	116.94	97	177.88	80	238.83	63	299.77		
42	57.41	25	118.36	8	179.30	245	240.24	228	301.19		
207	58.83	190	119.78	173	180.72	156	241.66	139	302.61		
118	60.25	101	121.19	84	182.14	67	243.08	50	304.03		

Table 10 : Equator Crossing Longitudes (in order of Longitude)

2.4.4. The Jason-3 Project Phases

The satellite mission has two main phases: verification and operational.

2.4.4.1. The verification phase

The calibration/validation phase (9 months) began shortly after launch, when the satellite reached the operational (nominal repetitive) orbit and the satellite and sensor systems were functioning normally. This phase continued until the data received from the sensors were satisfactorily calibrated and verified.

During this calibration/validation phase, the quality control will be achieved through many steps as a series of quality controls designed to ensure a continuous supply of data : regular cyclic data product analysis (complete parameter analysis and diagnostics, missions/edited measurements, crossovers and along-track analysis, orbit analysis, ...), cross-calibration with other altimeters (Jason-2, SARAL/AltiKa,...), instrumental expertise for altimeter and radiometer monitoring, and by performing absolute calibration at dedicated *in situ* calibration sites.

This verification phase is divided in 2 phases which overlap:

1. One dedicated to the validation of the near real time products (OGDRs).
2. The second phase dedicated to the validation of the off-line products (IGDR and GDR).

2.4.4.2. The operational (routine and long-term CALVAL activities)

The operational phase begins after the successful validation of each product type, and when all necessary algorithm and processing changes are implemented to have Jason-3 performances at the



same level as other altimetric satellites. Beyond the CALVAL phase, it is necessary to perform regular long-term CALVAL in order to monitor biases and drifts of Jason-3 overall system: in addition to previously mentioned analysis, comparison of Jason-3 data with global and regional networks of *in situ* data (tide gauges, T/S profiles, ...) will be performed as soon as enough *in situ* data are available (~1 year after launch). These different analyses will also be implemented in order to calibrate and validate new ground processing algorithms that could be proposed and implemented during the CALVAL phase.

2.5. Data Processing and Distribution

Processing centers perform functions such as science data processing, data verification and orbit determination.

There are three levels of processed data:

- Telemetry data (raw data or level0)
- Sensor Data Records (engineering units or level1)
- Geophysical Data Records (geophysical units or level2)

There are two kinds of data processing and distribution:

- **Real-time processing and distribution** (EUMETSAT and NOAA)

The operational geophysical data record (OGDR) is available with a latency of 3-5 hours. Note that this is a non-validated product that uses orbits computed by the on-board DORIS Navigator (DIODE) and that it does not contain all the environmental/geophysical corrections.

- **Delayed-mode processing (CNES) and distribution** (CNES and NOAA)

The interim geophysical data record (IGDR) is available per pass with a latency of 2 days. Note that this is not a fully validated product, although it uses a preliminary orbit and includes all the environmental/geophysical corrections (preliminary for some of them).

The geophysical data record (GDR) is a fully validated product that uses a precise orbit and the best environmental/geophysical corrections. This product is available per repeat cycle with a latency of 90 days. Validation is performed by two teams at CNES and NASA/JPL to ensure in depth validation.

Geophysical data records are disseminated to users as they become available, as well as ingested in two main archives (at CNES and NOAA), where they are made available to the scientific community.

The NRT and offline data are provided through different sources and means as discussed below. Note that the telemetry acquisition strategy, designed to minimize the risk of science data loss, sometimes results in files containing data which overlaps in time. The NRT ground processing does not remove these overlaps, so it is possible to encounter two or more OGDR products which have overlapping start and stop sensing times. CNES-EUMETSAT-NOAA centers are disseminating Jason-3 products according to the interagency agreement.

- **CNES via AVISO+ data services** : <http://www.aviso.altimetry.fr>

“Archiving, Validation and Interpretation of Satellite Oceanographic data” is the French multi-satellite data distribution center dedicated to space oceanography, developed by CNES.

AVISO+ distributes and archives Jason-3 delayed-time data ((I)GDR).

- **EUMETSAT**: <http://www.eumetsat.int>

EUMETSAT is the European Organisation for the Exploitation of Meteorological Satellites. Its role is to deliver weather and climate-related satellite data, images and products- 24 hours a day, 365 days a year.



EUMETSAT distributes operational data (OGDR)

- NOAA: <http://www.noaa.gov>

The mission of the US National Oceanic and Atmospheric Administration is to understand and predict changes in Earth's environment and conserve and manage coastal and marine resources to meet USA's economic, social, and environmental needs

NOAA distributes operational data, and distributes and archives delayed-time data ((O)(I)GDR)

2.5.1. Access to NRT data

The OGDR, OGDR-SSHA, and OGDR-BUFR files are produced at NOAA and EUMETSAT. Telemetry data downlinked to NOAA's ground stations at Wallops, VA and Fairbanks, AK are used to produce NOAA OGDR products, while telemetry data downlinked to the EUMETSAT earth terminal at Usingen, Germany are used to produce EUMETSAT OGDRs. NOAA and EUMETSAT exchange their products so that both agencies have a complete set.

In near real time, NOAA disseminates the complete set of OGDR files via ftp and EUMETSAT disseminates the complete set of OGDR files on EUMETCast. The complete set of OGDR files consists of OGDR, OGDR-SSHA and OGDR-BUFR, both generated at EUMETSAT and NOAA.

Note that the OGDR-BUFR files available from NOAA/NCEI use a filename similar to the native and reduced-SSHA filenames, beginning with 'JA3_OPB'. The UMARF archive at EUMETSAT utilizes the WMO/GTS filenames indicated above, beginning with 'W_US' for NOAA OGDR-BUFR files and 'W_XX' for the EUMETSAT generated OGDR-BUFR files.

The OGDR-BUFR data are additionally available in near real-time from the Global Telecommunications System (GTS). NOAA and EUMETSAT inject only their own OGDR-BUFR files onto GTS, to avoid duplication.

Details on data dissemination services from NOAA and EUMETSAT agencies are described below.

2.5.2. Access to off-line data

The IGDR and GDR families of files are produced solely by CNES, and are available to users from NOAA's National Centers for Environmental Information (NCEI; <https://www.ncei.noaa.gov/products/jason-satellite-products>), and from the French Archiving, Validation, and Interpretation of Satellite Oceanographic data (AVISO; <http://www.aviso.altimetry.fr>) ftp server. Both of these archival facilities also provide a variety of auxiliary files used to produce the O/I/GDR datasets, and NOAA also provides the OGDR family of datasets.

Data dissemination services from NOAA and CNES agencies are described below.

2.5.3. Documentation

This Jason-3 User's Handbook document describes only the native product format. A description of the O/I/GDR product format and contents is provided in the CNES document "SALP-ST-M-EA-16122-CN: SALP Products Specification - Volume 30: Jason-3 User Products". All documents are available through the data dissemination services.

A BUFR reading software library can be obtained from:
<https://confluence.ecmwf.int/display/ECC/Releases>



2.6. Access to data via NOAA

2.6.1. Access to NRT data

Individual users who require science data in near-real-time can access the O/I/GDR at the National Centers for Environmental Information (NCEI): <https://www.ncei.noaa.gov/products/jason-satellite-products>. Supported access methods include direct ftp, http, and OPeNDAP and THREDDS. Helpdesk support is available via NCEI.info@noaa.gov. The NCEI Satellite Oceanography team can help users create subscriptions to specified data streams as well as provide access to ancillary, auxiliary, orbital and other types of Jason-3 data.

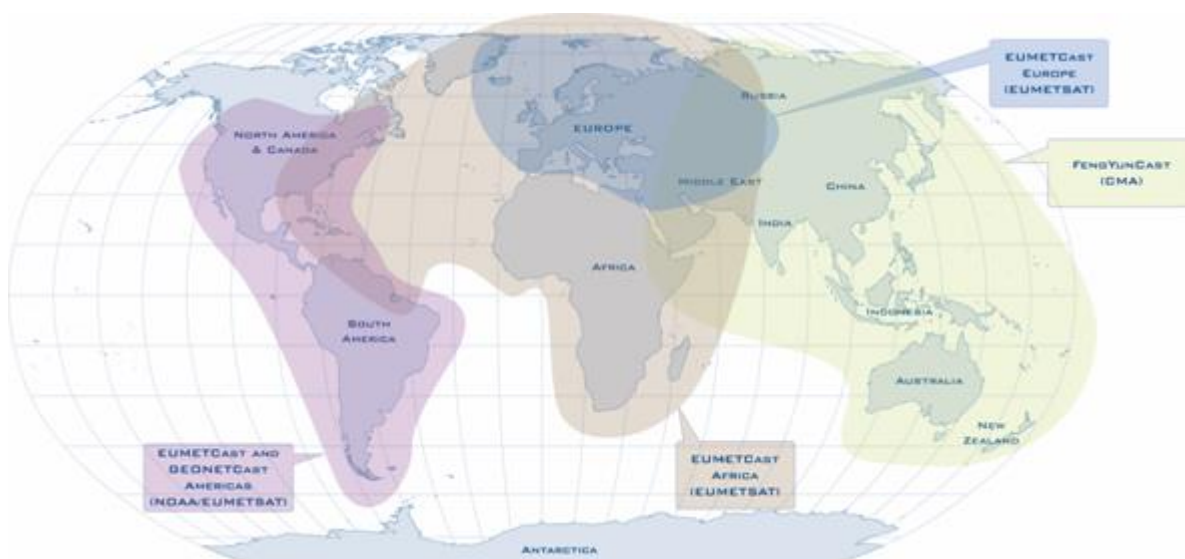
Operational users who demonstrate a need for minimum latency near real-time access will need to register with NOAA's Product Distribution & Access server (PDA). Please contact the PDA administrator (PDA_Administrator@noaa.gov) to determine if PDA access is needed for your use. Online registration will be provided once approval has been given to use the PDA.

2.7. Access to data via EUMETSAT

2.7.1. NRT data access

Operational users requiring near real-time access (within a few hours of acquisition) can receive data via EUMETCast, which is the prime dissemination mechanism for EUMETSAT satellite data and meteorological products. EUMETCast is also used to deliver data supplied by several external data providers.

EUMETCast is an environmental data and product dissemination system based on standard Digital Video Broadcast (DVB) technology. It uses commercial telecommunication geostationary satellites to broadcast data and products to a wide user community. EUMETSAT operates three EUMETCast broadcasts: EUMETCast Europe in Ku-band via Hotbird-6 EUMETCast Africa in C-band via AtlanticBird-3 and EUMETCast South America in C-band via NewSkies-806. The coverage zones of these broadcasts are shown in Figure below. The Jason-3 OGDR products are currently disseminated over all beams.





GEONETCast Coverage Zones

EUMETCast is part of a wider data dissemination cooperation network known as GEONETCast, defined as a global network of satellite based data dissemination systems providing environmental data to a world-wide user community. The current partners within the GEONETCast initiative include the National Oceanic and Atmospheric Administration (NOAA), the World Meteorological Organization (WMO) and EUMETSAT, as well as many prospective data provider partners.

EUMETCast is a multi-service dissemination mechanism and other environmental data streams and products are also delivered via EUMETCast :

- Space-based observations from the Meteosat, Metop, GOES, MT-SAT and FY2 satellites - at their most frequent, these data are delivered to Users within 5-minutes of processing
- MODIS level 1 and 2 products covering selective geographical regions
- Numerical Weather Forecasts
- In-situ observational data
- Land application products covering Europe, Africa and South America
- Marine meteorological and ocean surface products covering the Atlantic, Mediterranean Sea and Yellow Sea
- Atmospheric chemistry products

EUMETCast has an installed user base of over 2500 stations worldwide.

A typical EUMETCast reception station comprises a standard PC with DVB card inserted and a satellite off-set antenna fitted with a digital universal V/H LNB. All components of the reception station are commercially available. The hardware costs for a single PC station for EUMETCast Europe (Ku-band) reception start at around €1,500. In addition, EUMETCast Client Software package is required for handling the incoming DVB and storing it as data files. This package is available directly from EUMETSAT at a one of fee of €100 and forms part of any registration process.

Further information on EUMETCast can be found on the EUMETSAT Web site at:

http://www.eumetsat.int/Home/Main/What_We_Do/EUMETCast/index.html?l=en or alternatively follow the links to 'What We Do'-'EUMETCast'. Note that the coverage of EUMETCast is achieved through different beams, and the user location will determine the technical requirements of the EUMETCast reception station equipment.

The Jason-3 products available via EUMETCast are the EUMETSAT and NOAA injected OGDR, OGDR-SSHA and OGDR-BUFR. To access these on EUMETCast, users are requested to register online via the EUMETSAT Web site, or to contact the EUMETSAT User Service Helpdesk. As for Jason-2 near real-time products, already disseminated by EUMETSAT via EUMETCast, the Jason-3 products will be disseminated on all EUMETCast channels (Europe, Americas and Africa).

All enquiries related to EUMETCast can be addressed to the EUMETSAT User Helpdesk, email ops@eumetsat.int, who will be happy to assist with information on reception station manufacturers, reception station setup and data access registration to the Jason-3 service, or indeed to other near real-time EUMETSAT data services.

2.7.2. Access to archived data

The Jason-3 products generated and distributed by EUMETSAT in near real-time (i.e., OGDR, OGDR-SSHA and OGDR-BUFR) are also archived in the multi-mission EUMETSAT Archive. Any user can access Jason-3 data from the EUMETSAT archive upon registration. Information on registration, the archive itself and how to use it can be found at <http://archive.eumetsat.org/umarf> or follow the links to 'Access to Data' and then 'Archive Service'. Data delivery media include, among others, direct ftp push to a provided IP address, including the possibility of establishing standing orders, or



download by the user from an html page. Note however that this is not a near real-time data access, but that it can take up to several hours and occasionally even days to get the data.

2.8. Access to OGDR-BUFR files data on GTS

All of the OGDR-BUFR data, whether injected by NOAA or EUMETSAT, will appear on the World Meteorological Organization's GTS network. End users with a GTS presence (typically large meteorological agencies) can retrieve the data by keying on the WMO/GTS headers specific to the Jason-3 data: 'ISZX01 KNES' for NOAA OGDR-BUFR files, and 'ISZX01 EUMS' for EUMETSAT OGDR-BUFR files. The original files are comprised of approximately 15 minute BUFR 'messages' which will appear separately on the GTS.

It is also possible to scour the NOAA National Weather Service's GTS ftp server for the individual messages, by searching for 'ISZX01' strings. At this time, the OGDR-BUFR messages have been appearing at the following location, but future access at this specific site cannot be guaranteed:

<http://tgftp.nws.noaa.gov/SL.us008001/DF.bf/DC.sfsat/DS.qscat>

2.9. CNES data distribution

2.9.1. Details of off line data access via CNES

Off line IGDR and GDR products via Aviso+ ftp portal with an authenticated access (<ftp://ftp-access.aviso.altimetry.fr/>).

.

Registration is needed : <https://www.aviso.altimetry.fr/en/data/data-access/registration-form.html> and select the products

- "GDR / IGDR (Geophysical Data Records)" and/or
- "Waveform (Radar return echoes in Sensor Geophysical Data Records)" and/or
- "Wind / Wave Along-track from Geophysical Data Records (L2)",

depending on the way you use them.

A login/password are provided .

Home directory : /geophysical-data-record/jason-3

With the following ftp server directory tree:

documentation	→	directory containing product spec, product handbook, reading tools, ...
igdr	→	directory containing IGDR native products (with a sub directory for each cycle and sub directory containing the latest data)
sigdr	→	directory containing S-IGDR (with a unique sub directory containing the latest data)
ssha_igdr	→	directory containing IGDR reduced products (with a sub directory for each cycle and a sub directory containing the latest data)
gdr_d *	→	directory containing GDR native products (with a sub directory for each cycle)
sgdr_d *	→	directory containing S-GDR (with a sub directory for each cycle)



ssha_gdr_d *	→	directory containing GDR reduced products (with a sub directory for each cycle)
gdr_d_validation_report *	→	directory containing GDR validation reports
gdr_f **	→	directory containing GDR-F native products (with a sub directory for each cycle)
sgdr_f **	→	directory containing S-GDR-F (with a sub directory for each cycle)
ssha_gdr_f **	→	directory containing GDR-F reduced products (with a sub directory for each cycle)
gdr_f_validation_report	→	directory containing GDR-F validation reports

*All products in standard d will be deleted after the end of the GDR-F reprocessing

**For standard F , Zip format is given up

For any questions on Jason-3 data dissemination on AVISO+ servers please contact:

aviso@altimetry.fr

3. Product evolution history

3.1. Models and Standards History

3.1.1. Models and Standards on Version “T” products

The version of the data produced during the Cal/Val phase of the mission is identified by the version letter “T” in the name of the data products. This “T” calibration/validation version will be extensively validated by PIs during the verification phase.

The “T” product version adopts models and standards that are consistent with version “d” of the Jason-2 (I)GDR products (see RD 1).

The table below summarizes the models and standards that are adopted in this version of the Jason-3 (O)(I)GDRs. Section 3.2 provides more details on some of these models.

Model	Product Version “T”
Orbit	Based on Doris onboard navigator solution for OGDRs. DORIS tracking data for IGDRs (orbit standard “POE-E”). DORIS and/or SLR and/or GPS tracking data for GDRs (orbit standard “POE-E”).
Altimeter Retracking	“Ocean MLE4” retracking MLE4 fit from 2 nd order Brown analytical model : MLE4 simultaneously retrieves the 4 parameters that can be inverted from the altimeter waveforms: - Epoch (tracker range offset) ⇒ altimeter range



Model	Product Version “T”
	<ul style="list-style-type: none"> - Composite Sigma \Rightarrow SWH - Amplitude \Rightarrow Sigma0 - Square of mispointing angle (Ku band only, a null value is used in input of the C band retracking algorithm) <p>“Ocean MLE3” retracking MLE3 fit from 1st order Brown analytical model : MLE3 simultaneously retrieves the 3 parameters that can be inverted from the altimeter waveforms:</p> <ul style="list-style-type: none"> - Epoch (tracker range offset) \Rightarrow altimeter range - Composite Sigma \Rightarrow SWH - Amplitude \Rightarrow Sigma0 <p>“Ice” retracking Geometrical analysis of the altimeter waveforms, which retrieves the following parameters:</p> <ul style="list-style-type: none"> - Epoch (tracker range offset) \Rightarrow altimeter range - Amplitude \Rightarrow Sigma0
Altimeter Instrument Corrections	Two sets: <ul style="list-style-type: none"> - one set consistent with MLE4 retracking - one set consistent with MLE3 retracking
Jason-3 Advanced Microwave Radiometer (AMR) Parameters	Using calibration parameters derived from long term calibration tool developed and operated by NASA/JPL
Dry Troposphere Range Correction	From ECMWF atmospheric pressures and model for S1 and S2 atmospheric tides
Wet Troposphere Range Correction from Model	From ECMWF model
Ionosphere correction	From Ku/C range differences
Ionosphere model correction	Based on Global Ionosphere TEC Maps from JPL
Sea State Bias	Two empirical models: <ul style="list-style-type: none"> - MLE4 version derived from 1 year of MLE4 Jason-2 altimeter data with version "d" geophysical models - MLE3 version derived from 1 year of MLE3 Jason-2 altimeter data with version "d" geophysical models
Mean Sea Surface	MSS_CNES-CLS11
Mean Dynamic Topography	MDT_CNES-CLS09
Geoid	EGM96
Bathymetry Model	DTM2000.1
Inverse Barometer Correction	Computed from ECMWF atmospheric pressures after removing S1 and S2 atmospheric tides
Non-tidal High-frequency Dealiasing Correction	Mog2D High Resolution ocean model on (I)GDRs. None for OGDRs. Ocean model forced by ECMWF atmospheric pressures after removing S1 and S2 atmospheric tides
Tide Solution 1	GOT4.8 + S1 ocean tide. S1 load tide ignored
Tide Solution 2	FES2004 + S1 and M4 ocean tides. S1 and M4 load tides ignored
Equilibrium long-period ocean tide model	From Cartwright and Taylor tidal potential
Non-equilibrium long-period ocean tide model	Mm, Mf, Mtm, and Msqm from FES2004
Solid Earth Tide Model	From Cartwright and Taylor tidal potential
Pole Tide Model	Equilibrium model
Wind Speed from Model	ECMWF model
Altimeter Wind Speed Model	Derived from Jason-1 data



Model	Product Version “T”
Rain Flag	Derived from comparisons to thresholds of the radiometer-derived integrated liquid water content and of the difference between the measured and the expected Ku-band backscatter coefficient
Ice Flag	Derived from comparison of the model wet tropospheric correction to a dual-frequency wet tropospheric correction retrieved from radiometer brightness temperatures, with a default value issued from a climatology table

Table 11 : Models and standards (Jason-3 Product Version “T”)

3.1.2. Models and Standards on Version “D” products

The “D” GDR Standard was introduced in September 2016 (cycle 22) at the end of the Cal/Val phase of the mission (related to CNES internal change requests SALP-FT-8044, SALP-FT-8377 and SALP-FT-8477).

In September 2018, GDR-D Standard was updated with the use of POE-F orbit standard.

Model	Product Version “D”
Reference Ellipsoid	Topex/Poseidon
Orbit	Based on Doris onboard navigator solution for OGDRs. DORIS tracking data for IGDRs (orbit standard “POE-E”). DORIS and/or SLR and/or GPS tracking data for GDRs (orbit standard “POE-E”). Orbit Standard POE-F since September 2018 (cycle 95)
Altimeter Retracking	<p>“Ocean MLE4” retracking MLE4 fit from 2nd order Brown analytical model : MLE4 simultaneously retrieves the 4 parameters that can be inverted from the altimeter waveforms:</p> <ul style="list-style-type: none"> - Epoch (tracker range offset) ⇒ altimeter range - Composite Sigma ⇒ SWH - Amplitude ⇒ Sigma0 - Square of mispointing angle (Ku band only, a null value is used in input of the C band retracking algorithm) <p>“Ocean MLE3” retracking MLE3 fit from 1st order Brown analytical model : MLE3 simultaneously retrieves the 3 parameters that can be inverted from the altimeter waveforms:</p> <ul style="list-style-type: none"> - Epoch (tracker range offset) ⇒ altimeter range - Composite Sigma ⇒ SWH - Amplitude ⇒ Sigma0 <p>“Ice” retracking Geometrical analysis of the altimeter waveforms, which retrieves the following parameters:</p> <ul style="list-style-type: none"> - Epoch (tracker range offset) ⇒ altimeter range - Amplitude ⇒ Sigma0
Altimeter Instrument Corrections	Two sets: - one set consistent with MLE4 retracking - one set consistent with MLE3 retracking
Jason-3 Advanced Microwave Radiometer (AMR) Parameters	Using calibration parameters derived from long term calibration tool developed and operated by NASA/JPL
Dry Troposphere Range	From ECMWF atmospheric pressures and model for S1 and S2



Model	Product Version “D”
Correction	atmospheric tides
Wet Troposphere Range Correction from Model	From ECMWF model
Ionosphere correction	From Ku/C range differences
Ionosphere model correction	Based on Global Ionosphere TEC Maps from JPL
Sea State Bias	Two empirical models: <ul style="list-style-type: none"> - MLE4 version derived from 1 year of MLE4 Jason-2 altimeter data with version "d" geophysical models - MLE3 version derived from 1 year of MLE3 Jason-2 altimeter data with version "d" geophysical models
Mean Sea Surface	MSS_CNES-CLS11
Mean Dynamic Topography	MDT_CNES-CLS09
Geoid	EGM96
Bathymetry Model	DTM2000.1
Inverse Barometer Correction	Computed from ECMWF atmospheric pressures after removing S1 and S2 atmospheric tides
Non-tidal High-frequency Dealiasing Correction	Mog2D High Resolution ocean model on (I)GDRs. None for OGDRs. Ocean model forced by ECMWF atmospheric pressures after removing S1 and S2 atmospheric tides
Tide Solution 1	GOT4.8 + S1 ocean tide. S1 load tide ignored
Tide Solution 2	FES2004 + S1 and M4 ocean tides. S1 and M4 load tides ignored
Equilibrium long-period ocean tide model	From Cartwright and Taylor tidal potential
Non-equilibrium long-period ocean tide model	Mm, Mf, Mtm, and Msqm from FES2004
Solid Earth Tide Model	From Cartwright and Taylor tidal potential
Pole Tide Model	Equilibrium model
Wind Speed from Model	ECMWF model
Altimeter Wind Speed Model	Derived from Jason-1 data
Rain Flag	Derived from comparisons to thresholds of the radiometer-derived integrated liquid water content and of the difference between the measured and the expected Ku-band backscatter coefficient
Ice Flag	Derived from comparison of the model wet tropospheric correction to a dual-frequency wet tropospheric correction retrieved from radiometer brightness temperatures, with a default value issued from a climatology table

Table 12 : Models and standards (Jason-3 Product Version "D")

3.1.3. Models and standards on Version "f" Products

The “f” product version brings major improvements to the previous version 'D' GDRs, adopts some new models, and accounts for inclusion of new fields improving the data quality.

The table below summarizes the models and standards that are adopted in this version of the (O)(I)GDRs.



Model	Product Version “f”
Reference Ellipsoid	WGS84
Orbit	Based on Doris onboard navigator solution for OGDRs. DORIS and/or GPS tracking data for IGDRs (orbit standard “POE-F”). DORIS and/or GPS tracking data for GDRs (orbit standard “POE-F”).
Altimeter Retracking	<p><u>“Ocean MLE4” retracking</u> MLE4 fit from 2nd order Brown analytical model : MLE4 simultaneously retrieves the 4 parameters that can be inverted from the altimeter waveforms:</p> <ul style="list-style-type: none"> - Epoch (tracker range offset) ⇒ altimeter range - Composite Sigma ⇒ SWH - Amplitude ⇒ Sigma0 - Square of mispointing angle (Ku band only, a null value is used in input of the C band retracking algorithm) <p><u>“Ocean MLE3” retracking</u> MLE3 fit from 1st order Brown analytical model : MLE3 simultaneously retrieves the 3 parameters that can be inverted from the altimeter waveforms:</p> <ul style="list-style-type: none"> - Epoch (tracker range offset) ⇒ altimeter range - Composite Sigma ⇒ SWH - Amplitude ⇒ Sigma0 <p><u>“Ice” retracking</u> Geometrical analysis of the altimeter waveforms, which retrieves the following parameters:</p> <ul style="list-style-type: none"> - Epoch (tracker range offset) ⇒ altimeter range - Amplitude ⇒ Sigma0 <p><u>“Adaptive” retracking</u> Adaptive retracking [Thibaut 2021] fit from Brown numerical model taking the real on-board PTR. Adaptive simultaneously retrieves the 4 parameters that can be inverted from the altimeter waveforms:</p> <ul style="list-style-type: none"> - Epoch (tracker range offset) ⇒ altimeter range - Composite Sigma ⇒ SWH - Amplitude ⇒ Sigma0 - Gamma
Altimeter Instrument Corrections	Two sets: <ul style="list-style-type: none"> - one set consistent with MLE4 retracking - one set consistent with MLE3 retracking No set needed for adaptive retracking
Jason-3 Advanced Microwave Radiometer (AMR) Parameters	Using calibration parameters derived from long term calibration tool developed and operated by NASA/JPL
Dry Troposphere Range Correction	From ECMWF atmospheric pressures and model for S1 and S2 atmospheric tides. 2 solutions: integration from sea surface level or from estimated measurement altitude using DEM (O/IGDR) or altimetry range (GDR).
Wet Troposphere Range Correction from Model	From ECMWF model. 2 solutions: integration from DEM or using altimetry range.
Ionosphere correction	Two solutions: <ul style="list-style-type: none"> -from Ku/C range differences correction -from Ku/C range differences filtered correction
Ionosphere model correction	Based on Global Ionosphere TEC Maps from JPL



Model	Product Version “f”
Sea State Bias	CLS empirical solutions fitted on one year of Jason-3 GDR-F data [Tran, 2019] Two solutions for each retracking (MLE4 and Adaptive): - 2D model from SWH and altimeter wind-speed (standard version) - 3D model from SWH, altimeter wind-speed and t02 mean wave period from model (improved version)
Mean Sea Surface	2 Solutions: MSS_CNES-CLS15 MSS_DTU_2018
Mean Dynamic Topography	MDT_CNES-CLS18
Geoid	EGM2008
Bathymetry Model	ACE2 (from EAPRS Laboratory)
Inverse Barometer Correction	Computed from ECMWF atmospheric pressures after removing S1 and S2 atmospheric tides
Non-tidal High-frequency Dealiasing Correction	Mog2D High Resolution ocean model. Ocean model is forced by ECMWF wind field and atmospheric pressure after removing S1 and S2 atmospheric tides
Tide Solution 1	GOT4.10c
Tide Solution 2	FES2014b
Equilibrium long-period ocean tide model	From tidal potential of [Cartwright, 1973]
Non-equilibrium long-period ocean tide model	Mm, Mf, Mtm, MSqm, Sa and Ssa from FES2014b
Solid Earth Tide Model	From tidal potential of [Cartwright, 1973]
Pole Tide Model	From [Desai, 2015] and MPL [Desai, 2017]
Internal Tide Model	From [Zaron, 2019]
Wind Speed from Model	ECMWF model
Altimeter Wind Speed Model	Following Gourrion’s approach [Gourrion, 2000] , based on Collard’s model computed from Jason-1 data [Collard, 2005]
Rain Flag	Derived from comparisons to thresholds of the radiometer-derived integrated liquid water content and of the difference between the measured and the expected Ku-band backscatter coefficient
Ice Flag	Derived from comparison of the model wet tropospheric correction to a dual-frequency wet tropospheric correction retrieved from radiometer brightness temperatures, with a default value issued from a climatology table

Table 13: Models and standards (Jason-3 Product Version “F”)

3.2. Models and Editing on Version “F” Products

3.2.1. Orbit models

Jason-3 orbit standards are based on version “POE-F” orbit model. Its characteristics are summarized below. Previous standard used on Jason-3 mission (POE-E) is also recalled:

	POE-E	POE-F



Jason-3 Products Handbook

Iss :2.1 - date : June 21^h , 2021



36

Gravity model	EIGEN-GRGS.RL03-v2.MEAN-FIELD	EIGEN-GRGS.RL04-v1.MEAN-FIELD
Surface forces	<p>Non-tidal TVG: one annual, one semi-annual, one bias and one drift terms for each year up to deg/ord 80; C21/S21 modeled according to IERS2010 conventions</p> <p>Solid Earth tides: from IERS2003 conventions</p> <p>Ocean tides: FES2012</p> <p>Oceanic/atmospheric gravity: 6hr NCEP pressure fields (70x70) + tides from Biancale-Bode model</p> <p>Pole tide: solid Earth and ocean from IERS2010 conventions</p> <p>Third bodies: Sun, Moon, Venus, Mars and Jupiter</p>	<p>Non-tidal TVG: one annual, one semi-annual, one bias and one drift terms for each year up to deg/ord 90; C21/S21 non modified</p> <p>Unchanged</p> <p>Ocean tides: FES2014</p> <p>Oceanic/atmospheric gravity: 3hr dealiasing products from GFZ AOD1B RL06</p> <p>Unchanged</p> <p>Unchanged</p>
Estimated dynamical parameters	Stochastic solutions	Unchanged
Satellite reference	<p>Mass and center of gravity: post-launch values + variations generated by Control Center</p> <p>Attitude model:</p> <p>For Jason satellites: quaternions and solar panel orientation from control center, completed by nominal yaw steering law when necessary</p> <p>Other satellites: nominal attitude law</p>	<p>Unchanged</p> <p>Refined nominal attitude laws</p>



Jason-3 Products Handbook

Iss :2.1 - date : June 21^h , 2021



37

<p>Displacement of reference points</p>	<p>Earth tides: IERS2003 conventions</p> <p>Ocean loading: FES2012</p> <p>Pole tide: solid earth pole tides and ocean pole tides (Desai, 2002), cubic+linear mean pole model from IERS2010</p> <p>S1-S2 atmospheric pressure loading, implementation of Ray & Ponte (2003) by van Dam</p> <p>Reference GPS constellation: JPL solution - fully consistent with IGS08</p>	<p>Unchanged</p> <p>Ocean loading: FES2014</p> <p>Pole tide: solid earth pole tides and ocean pole tides (Desai, 2002), new linear mean pole model</p> <p>Unchanged</p> <p>Reference GPS constellation: GRG solution - fully consistent with IGS14</p>
<p>Geocenter variations</p>	<p>Tidal: ocean loading and S1-S2 atmospheric pressure loading</p> <p>Non-tidal: seasonal model from J. Ries, applied to DORIS/SLR stations</p>	<p>Unchanged</p> <p>Non-tidal: full non-tidal model (semi-annual, annual, inter-annual) derived from DORIS data and the OSTM/Jason-2 satellite, applied to DORIS/SLR stations and GPS satellites</p>
<p>Terrestrial Reference Frame</p>	<p>Extended ITRF2008 (SLRF/ITRF2008, DPOD2008, IGS08)</p>	<p>Extended ITRF2014 (SLRF/ITRF2014, DPOD2014, IGS14)</p>
<p>Earth orientation</p>	<p>Consistent with IERS2010 conventions and ITRF2008</p>	<p>Consistent with IERS2010 conventions and ITRF2014</p>
<p>Propagations delays</p>	<p>SLR troposphere correction: Mendes-Pavlis</p> <p>SLR range correction: constant 5.0 cm range correction for Envisat, elevation dependent range correction for Jason</p> <p>DORIS troposphere correction: GPT/GMF model</p> <p>DORIS beacons phase center correction</p> <p>GPS PCO/PCV (emitter and receiver) consistent with constellation orbits and clocks (IGS08 ANTEX), pre-launch GPS receiver phase map</p> <p>GPS: phase wind-up correction</p>	<p>Unchanged</p> <p>SLR range correction: geometrical models for all satellites</p> <p>DORIS troposphere correction: GPT2/VMF1 model</p> <p>Unchanged</p> <p>GPS PCO/PCV (emitter and receiver) consistent with constellation orbits and clocks (IGS14 ANTEX), in-flight adjusted GPS receiver phase map</p> <p>Unchanged</p>



<p>Estimated measurement parameters</p>	<p>DORIS: one frequency bias per pass, one troposphere zenith bias per pass</p> <p>SLR: Reference used to evaluate orbit precision and stability</p> <p>GPS: floating ambiguity per pass, receiver clock adjusted per epoch</p>	<p>DORIS: one frequency bias and drift (for “SAA stations”) per pass, one troposphere zenith bias per pass, horizontal tropospheric gradients per arc</p> <p>Unchanged</p> <p>GPS: fixed ambiguity (when possible) per pass, receiver clock adjusted per epoch</p>
<p>Tracking Data corrections</p>	<p>Jason-1 Doris data: updated South Atlantic Anomaly model (J.-M. Lemoine et al.) applied before and after DORIS instrument change</p> <p>DORIS time-tagging bias for Envisat and Jason aligned with SLR before and after instrument change</p>	<p>Unchanged</p> <p>Unchanged</p>
<p>Doris Weight</p>	<p>1.5 mm/s (1.5 cm over 10 sec)</p> <p>For Jason-1, SAA DORIS beacons weight is divided by 10 before DORIS instrument change</p>	<p>Process data down to as low elevation angles as possible (from 10° to 5° elevation cut-off angle) with a consistent down-weighting law</p> <p>Unchanged</p>
<p>SLR Weight</p>	<p>15 cm</p> <p>Reference used to evaluate orbit precision and stability</p>	<p>Unchanged</p>
<p>GPS Weight</p>	<p>2 cm (phase) / 2 m (code)</p>	<p>Unchanged</p>

Table 14. POE-E/POE-F orbit standard

3.2.2. Mean Sea Surface

3.2.2.1. MSS_CNES-CLS15

The MSS_CNES-CLS15 model is computed from 16 years of satellite altimetry data from a variety of missions. Its main characteristics are the following :

Name	MSS_CNES-CLS15
Reference ellipsoid	T/P
Referencing time period	1993-2013 (20 years)
Spatial coverage	Global (80°S to 84°N) - Oceanwide where altimetric data are available. Undefined on continents.
Spatial resolution	Regular grid with a 1/60° (1 minutes) spacing (i.e. ~2 km)
Grid	21600 points in longitude / 9841 points in latitude
MSS determination technique	Local least square collocation method on a 3' grid where altimetric data in a 200-km radius are selected. Estimation on a 1' grid based on SSH-Filtered MSS values (remove/restore technique to recover the full signal). The inverse method uses local anisotropic covariance functions which improve the shortest wavelengths.
Estimation error level	YES (in cm) - The Optimal Interpolation method provides a calibrated formal error
Altimetric dataset	T/P-J1-J2: 20 years mean profile (first orbit), T/P tandem & J1 tandem: 3.7 years profile GFO: 7 years mean profile ERS-2/EnviSat: 15 years mean profile, 1 year ERS-1 (geodetic phase) J1 & Cryosat-2: geodetic phase

Table 15 : MSS_CNES-CLS15 model characteristics

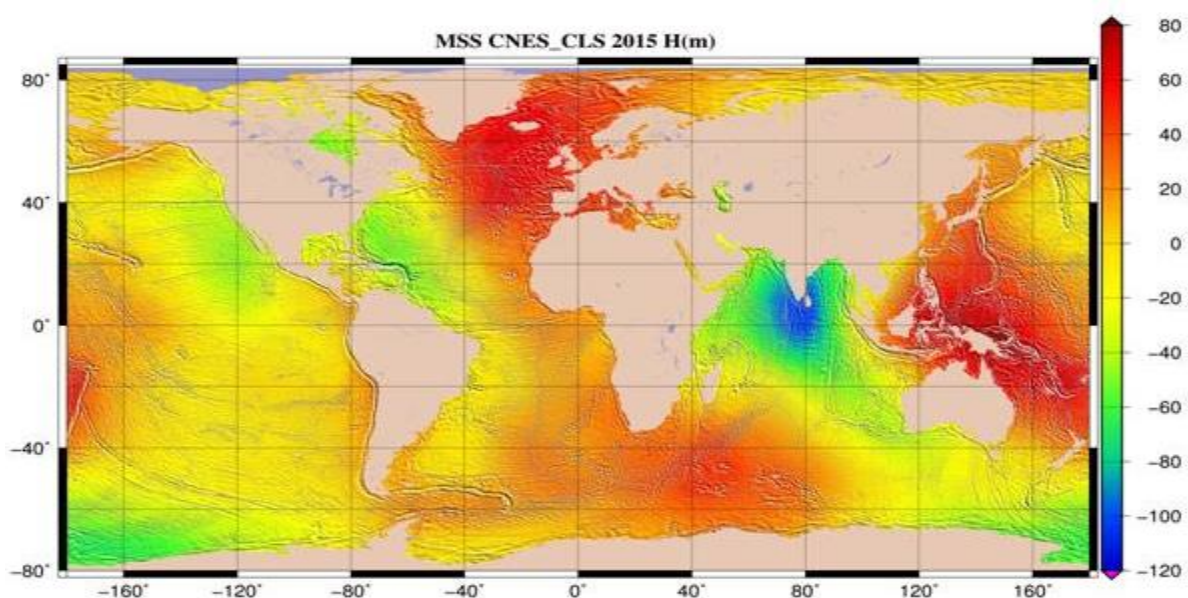


Figure 11 : Mean Sea Surface MSS_CNES-CLS15.



Refer to <http://www.aviso.altimetry.fr/en/data/products/auxiliary-products/mss/index.html> for more details on this model.

3.2.2.2. MSS_DTU-2018

Refer to :

Andersen, O., Knudsen, P., & Stenseng, L. (2018). A New DTU18 MSS Mean Sea Surface - Improvement from SAR Altimetry. 172. Abstract from 25 years of progress in radar altimetry symposium, Portugal.

ftp://ftp.space.dtu.dk/pub/DTU18/1_MIN/

3.2.3. Mean Dynamic Topography

The MDT_CNES-CLS09 model is computed from satellite altimetry data from a variety of missions. Its main characteristics are the following :

Name	MDT_CNES-CLS18
Referencing time period	1993-2012 (20 years)
Domain	Global - no Black Sea - no dedicated processing in the Arctic - the Med Sea come from the regional SOCIB MDT (Rio et al., 2014)
Spatial resolution	Regular grid with a 1/8°
Grid	2880 points in longitudes / 1440 points in latitude
MDT determination technique	Reference of the altimeter Sea Level Anomalies, computed relative to a 20 years (1993-2012) mean profile, in order to obtain absolute measurements of the ocean dynamic topography. Combined product based on GRACE and GOCE gravimetric data, altimetry and in situ data (hydrologic and drifters data)

Table 16 : MDT_CNES-CLS18 model characteristics

This sea surface height (mean sea surface height above geoid) corresponds to mean geostrophic currents and its changes.

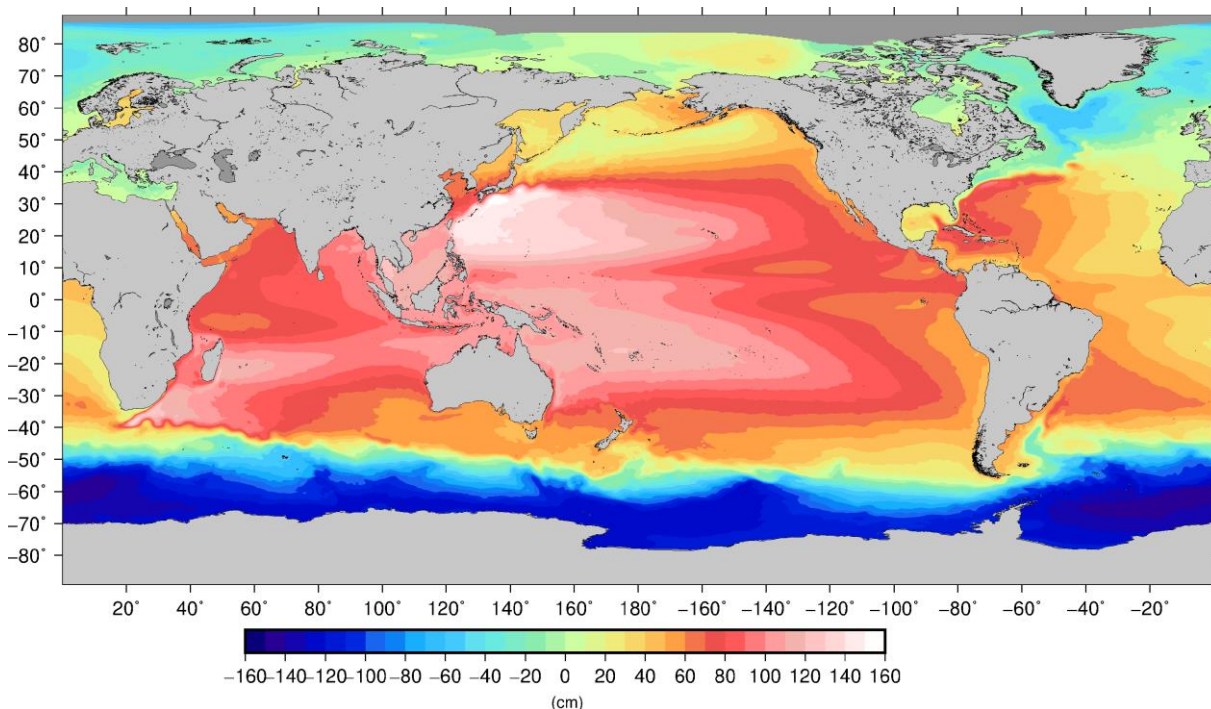


Figure 12 : Mean Dynamic Topography MDT_CNES-CLS18

Refer to <http://www.avisso.altimetry.fr/en/data/products/auxiliary-products/mdt/index.html> for more details on this model.

3.2.4. Geoid

Jason-3 (O)(I)GDRs use the EGM2008 geopotential to compute the geoid [Pavlis *et al.*, 2012].

EGM2008 is a spherical harmonic model of the Earth's gravitational potential, developed by a least squares combination of the ITG-GRACE03S gravitational model and its associated error covariance matrix. This grid was formed by merging terrestrial, altimetry-derived, and airborne gravity data.

The EGM2008 gravitational model has been used to calculate point values of geoid undulation on a 5 x 5 minute grid that spans the latitude range +90.0 deg. to -90.0 deg. The EGM2008 model is complete to spherical harmonic degree and order 2159 and contains additional coefficients up to degree 2190 and order 2159.

It has been corrected so as to refer to the reference ellipsoid (WGS84) and to add the permanent tide (zero frequency) [Rapp et al., 1991].

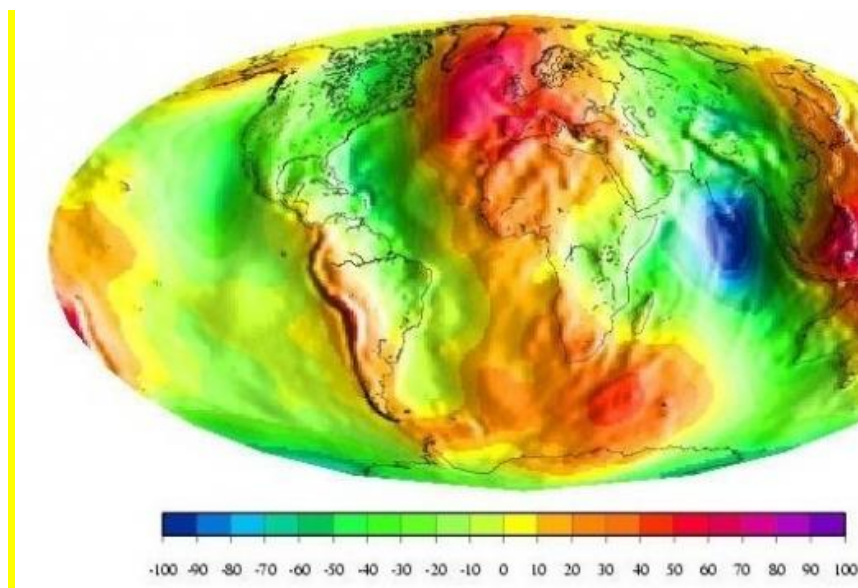


Figure 13 : EGM2008 geoid

More information on EGM08 can be found at <http://onlinelibrary.wiley.com/doi/10.1029/2011JB008916/full>

3.2.5. Bathymetry

The value of this parameter is determined from the ACE2 (Altimeter Corrected Elevations) digital elevation model at 30" resolution [Berry, P.A.M.; Smith,R.; Benveniste,J., 2008].

ACE2 digital elevation model has been created by synergistically merging the SRTM dataset with Satellite Radar Altimetry within the region bounded by $\pm 60N$.

Over the areas lying outside the SRTMs latitude limits other sources have been used such as including GLOBE and the original ACE DEM, together with new matrices derived from reprocessing the ERS1 Geodetic Mission dataset with an enhanced retracking system, and the inclusion of data from other satellites.

3.2.6. Ocean Tides

The two geocentric tide values provided on the Jason-3 (O)(I)GDR, `ocean_tide_got` and `ocean_tide_fes` are computed with diurnal and semidiurnal ocean and load tide values predicted by the GOT4.10c and FES2014b models, respectively.

Both geocentric ocean tide fields (`ocean_tide_got` and `ocean_tide_fes`) include the load tides from `load_tide_got` and `load_tide_fes` fields respectively, and the equilibrium long-period ocean tide



(ocean_tide_eq). The GOT4.10c model includes only one non-linear wave (M4), and FES2014b includes several non-linear waves: M4, M6, M8, MKS2, MN4, MS4, MSf, N4, S4.

Both models are interpolated to provide the geocentric ocean and load tides at the location of the altimeter measurement, and an interpolation quality flag is provided on the (O)(I)GDRs to indicate the quality of this interpolation (see ocean_tide_fes_interp_qual and ocean_tide_got_interp_qual).

3.2.6.1. GOT4.10c Ocean Tide Model

Solution GOT4.10c [Ray, 2013; Ray, personal communication], is the last version of GOT models developed by R. Ray.

This model is different from previous version GOT4.8 as it is now based on Jason-1 and Jason-2 data, ERS-1 and ERS-2 and GFO.

None T/P data has been used in this solution.

The solution consists of independent near-global estimates of 10 tidal constituents (Q1, O1, P1, S1, K1, N2, M2, S2, K2, M4) for both the oceanic and the loading tide components. An a priori model was used that consisted of the hydrodynamic model FES 2004 [Lyard et al. 2006] and several other local hydrodynamic models.

Note that GOT4.10c model uses the new tidal geocenter correction proposed by Shailen and Ray (2014). Moreover the dry-tropospheric correction used for the Jason satellites never had the S2 air-tide error that the original T/P data had.

GOT4.10c solution does not use the Cg correction, as it is a T/P correction.

GOT4.10c solution is provided on a 0.5° grid; moreover the ocean tide grids have been extrapolated on one pixel over coasts and ocean tide values are set to zero on lakes and enclosed-seas.

3.2.6.2. FES2014b Ocean Tide Model

FES2014 is the last version of the FES (Finite Element Solution) tide model developed in 2014-2016. It is an improved version of the FES2012 model, which was a fully revised version of the global hydrodynamic tide solutions initiated by the work of Christian Le Provost in the early nineties. This new FES2014 model has been developed, implemented and validated by the LEGOS, NOVELTIS and CLS, within a CNES funded project.

FES2014 takes advantage of longer altimeter time series and better altimeter standards, improved modelling and data assimilation techniques, a more accurate ocean bathymetry and a refined mesh in most of shallow water regions. Special efforts have been dedicated to address the major non-linear tides issue and to the determination of accurate tidal currents.

FES2014 is based on the resolution of the tidal barotropic equations (T-UGO model) in a spectral configuration.

A new global finite element grid (-2.9 million nodes, 50% more than FES2012) is used and model physic has been improved, leading to a nearly twice more accurate 'free' solution (independent of in situ and remote-sensing data) than the previous FES2012 version. Then the accuracy of this 'free' solution was improved by assimilating some long-term altimetry data (Topex/ Poseidon, Jason-1, Jason-2, TPN-J1N, and ERS-1 - ERS-2 - ENVISAT) and tidal gauges through an improved representer assimilation method.

A preliminary version, noted FES2014a, has been produced in 2015 based on GOT4v8ac loading tide. Then new tide loading effects have been computed using FES2014a oceanic tide (J.P. Boy, Univ. Strasbourg). These FES2014a tide loading effects have been used to produce the final model version noted FES2014b, which is used in Jason-3 GDR-F:

FES2014b geocentric (elastic) tide = FES2014b oceanic tide + FES2014a loading tide.

Final FES2014b solution shows strong improvement compared to FES2012 and GOT4V10, particularly in coastal and shelf regions and also in some deep ocean areas and in the Arctic region.



34 tidal constituents are available for both the oceanic tide and the loading tide components : 2N2, EPS2, J1, K1, K2, L2, La2, M2, M3, M4, M6, M8, Mf, MKS2, Mm, MN4, MS4, MSf, MSqm, Mtm, Mu2, N2, N4, Nu2, O1, P1, Q1, R2, S1, S2, S4, Sa, Ssa, T2.

FES2014b solution is provided on a $1/16^\circ$ grid; moreover the ocean tide grids have been extrapolated on ten pixels over coasts and ocean tide values are set to zero on lakes and enclosed-seas.

See "<http://www.aviso.altimetry.fr/en/data/products/auxiliary-products/global-tide-fes.html>" for more information.

3.2.7. Sea Surface Height Bias Recommendation

The Sea State Bias (SSB) can be defined as the difference between the apparent sea level as "seen" by the altimeter and the actual mean sea level. It is composed of: the Electromagnetic bias (EMB), and skewness and tracker biases that affect the accuracy of altimeter measurements and are all dependent on SWH. The EMB (main contributor) results from the fact that the radar senses an average sea surface lower than the true average sea surface, due to amplification from wave troughs. This bias can be expressed as a percentage of SWH, with the percentage being a complex function of the sea-surface slope and elevation statistical distribution.

Consolidated empirical SSB solutions have been developed from the Jason-3 measurements [Tran 2019]. They are provided in the form of table . The standard 2D version is expressed as a function of SWH and altimeter wind speed while the improved 3D version uses additionally a mean wave period estimate from wave model to better describe the local wave conditions.



3.2.8. Surface Classification Map

Jason-3 (O)(I)GDRs provides a 7 classes Surface Classification Flag (surface_classification_flag).

GDR-D	GDR-F
surface_type (4 classes)	surface_classification_flag (7 classes)
0: ocean 1: lake_enclosed_sea 2: ice 3: land	0:open_ocean 1:land 2:continental_water 3:aquatic_vegetation 4:continental_ice_snow 5:floating_ice 6:salted_basin

The map used for GDR-F Surface Classification consists in the combination of three data sources :

- GMT surface mask developed by Noveltis for the generation of the Jason-2 MNT (also including water body outlines from the LEGOS database)
- GLOBCOVER LC V2.0
- MODIS Mosaic of Antarctica from NSIDC

3.2.9. Coastal Distance & Angle of Approach to Coast

Coastal distance computation and angle of approach to coast determination is based on GSHHG_v2.3.7 model.

3.2.10. Global Slope Correction

Jason-3 (O)(I)GDRs use [Sandwell 3103] to compute the range reduction caused by the slope of the geoid relative to the ellipsoid.

This correction is NOT included in the ssha, and shall not be used with the mean sea surface (mean_sea_surface_cnescls or mean_sea_surface_dtu) provided in the product.

3.2.11. Data Editing Criteria

The following editing criteria are a recommended guideline for finding good records from the (O)(I)GDR to calculate the sea level anomaly from the Ku band range. The user should review these criteria before using them and may wish to modify them!

First, check the following conditions to retain only ocean data and remove any bad, missing, or flagged data:

Parameter	Value	Meaning
surface_classification_flag	0	Open oceans or semi-enclosed seas
ice_flag	0	No ice



Table 17 : Recommended editing criteria

Then, filter the data as follows to retain only the most valid data:

Parameter	Validity conditions
data01/ku/range_ocean_numval	$10 \leq x$
data01/ku/range_ocean_rms	$0 \leq x \text{ (mm)} \leq 200$
data01/altitude - data01/ku/range_ocean	$-130\ 000 \leq x \text{ (mm)} \leq 100\ 000$
data01/model_dry_tropo_cor_zero_altitude	$-2\ 500 \leq x \text{ (mm)} \leq -1\ 900$
data01/rad_wet_tropo_cor	$-500 \leq x \text{ (mm)} \leq -1$
data01/iono_cor_alt_filtered	$-400 \leq x \text{ (mm)} \leq 40$
data01/ku/sea_state_bias	$-500 \leq x \text{ (mm)} \leq 0$
data01/ocean_tide_fes	$-5\ 000 \leq x \text{ (mm)} \leq 5\ 000$
data01/solid_earth_tide	$-1\ 000 \leq x \text{ (mm)} \leq 1\ 000$
data01/pole_tide	$-15000 \leq x \text{ (mm)} \leq 15000$
data01/ku/swh_ocean	$0 \leq x \text{ (mm)} \leq 11\ 000$
data01/ku/sig0_ocean	$7 \leq x \text{ (dB)} \leq 30$
data01/wind_speed_alt	$-0 \leq x \text{ (m/s)} \leq 30$
data01/ku/off_nadir_angle_wf_ocean	$-0.2 \leq x \text{ (deg}^2\text{)} \leq 0.64$
data01/ku/sig0_ocean_rms	$x \text{ (dB)} \leq 1$
data01/ku/sig0_ocean_numval	$10 < x$

Table 18 : Recommended filtering criteria

To restrict studies to deep water, apply a limit, e.g., water depth of 1000m or greater, using the bathymetry parameter (ocean depth in meters.)



4. Using the (O)(I)GDR data

4.1. Overview

This section gives the reader a guide to the use of the Jason-3 (O)(I)GDR data. While this handbook tries to be correct and complete, note that nothing can replace the information to be gained at conferences and other meetings from those using these data. The reader must proceed with caution and at his or her own risk. Further information is also available on the web servers provided in Annex C, please direct questions and comments to the contacts given there.

The instruments on Jason-3 make direct observations of the following quantities: altimeter range, ocean significant wave height, ocean radar backscatter cross-section (a measure of wind speed), ionospheric electron content in the nadir direction, tropospheric water content, and position relative to the GPS satellite constellation. Ground based laser station and DORIS station measurements of the satellite location and speeds are used in precision orbit determination (POD). The DORIS stations also measure the ionospheric electron content along the line of sight to the satellite. All of these measurements are useful in themselves, but they are made primarily to derive the sea surface height with the highest possible accuracy. Such a computation also needs external data (not collected aboard Jason-3), e.g., atmospheric pressure, etc. In addition, instrument health and calibration data are collected onboard and used to make corrections to the main measurements and to monitor the instrument stability in the long term.

This (O)(I)GDR contains all relevant corrections needed to calculate the sea surface height. For the other "geophysical variables" in the (O)(I)GDR: ocean significant wave height, tropospheric water content, ionospheric electron content (derived by a simple formula), and wind speed, the needed instrument and atmospheric corrections have already been applied.

The following sections explain the rationale for how the corrections should be applied.

4.2. Typical computation from altimetry data

In this section references are made to specific (O)(I)GDR parameters by name using the name of the variable as described in the NetCDF data sets.

In addition with the MLE-4 retracking parameters, MLE-3 retracker parameters and Adaptive retracker parameters are also included in the Jason-3 products. Altimeter parameters (e.g. Range, swh, sigma0, etc) and related geophysical parameters (e.g. Ionosphere correction, sea state bias correction, wind speed, etc) named with no extension are derived from MLE-4 retracking, while those with the "mle3" extension are derived from MLE-3 retracking, and those with the "adaptive" extension are derived from Adaptive retracking.

Most users are advised to use the MLE-4 altimeter parameters for typical scientific applications. The MLE-3 Ku-band parameters are provided for the convenience of specialized studies on the calibration and validation of the mission and impact of altimeter retracking.

WARNING

Default values are given to data when computed values are not available (See [AD9]) so you must screen parameters to avoid using those with default values. Also you must check flag values. The related flags are given in the description of each variable (See [AD9]) although some discussion of flags appears in this section.



4.2.1. Corrected Altimeter Range

The main data of the (O)(I)GDR are the altimeter ranges. The (O)(I)GDR provides ranges measured at Ku band (ku/range_ocean, resp. ku/range_ocean_mle3 for MLE3, resp. ku/range_adaptive for Adaptive) and C band (c/range_ocean). The Ku band range is used for most applications. The given ranges are corrected for instrumental effects. These corrections are separately reported for each of the Ku (ku/range_cor_ocean_net_instr, resp. ku/range_cor_ocean_mle3_net_instr for MLE3, resp. ku/range_cor_adaptive for Adaptive) and C band ranges (c/range_cor_ocean_net_instr).

The given ranges must be corrected for path delay in the atmosphere through which the radar pulse passes and the nature of the reflecting sea surface. All range corrections are defined and they should be ADDED to the range. The corrected (Ku band) range is given by

$$\begin{aligned} \text{Corrected Range} = & \text{Range} + \text{Wet Troposphere Correction} \\ & + \text{Dry Troposphere Correction} \\ & + \text{Ionosphere Correction} \\ & + \text{Sea State Bias Correction} \end{aligned}$$

Wet Troposphere Correction :

Use AMR correction (rad_wet_tropo_cor).

Dry Troposphere Correction :

Use model correction (model_dry_tropo_cor_zero_altitude).

Ionosphere Correction :

Use MLE4 altimeter ionosphere filtered correction (iono_cor_alt_filtered) to correct Ku range issued from MLE4 retracking (ku/range_ocean).

Use MLE3 altimeter ionospheric filtered correction (iono_cor_alt_filtered_mle3) to correct Ku range issued from MLE3 retracking (ku/range_ocean_mle3).

Use Adaptive altimeter ionospheric filtered correction (iono_cor_alt_filtered_adaptive) to correct Ku range issued from Adaptive retracking (ku/range_adaptive).

Sea State Bias Correction :

Use MLE4 sea state bias correction (ku/sea_state_bias) to correct Ku range issued from MLE4 retracking (ku/range_ocean).

Use MLE3 sea state bias correction (ku/sea_state_bias_mle3) to correct Ku range issued from MLE3 retracking (ku/range_ocean_mle3).

Use Adaptive sea state bias correction (sea_state_bias_adaptive) to correct Ku range issued from Adaptive retracking (ku/range_adaptive).

Use improved version (sea_state_bias_3d_mp2) for fine regional studies

NOTE: The ionosphere and sea state bias corrections are both frequency dependent. Therefore Ku band corrections should only be applied to Ku band ranges, and C band corrections should only be applied to C band ranges. Section 4.2.4 explains how the C band ionosphere correction can be derived from the Ku band ionosphere correction (iono_cor_alt, resp. iono_cor_alt_mle3 for MLE3), while the C band sea state bias correction is provided as c/sea_state_bias (resp. c/sea_state_bias_mle3 for MLE3).

4.2.2. Sea Surface Height and Sea Level Anomaly

Sea surface height (SSH) is the height of the sea surface above the reference ellipsoid. It is calculated by subtracting the corrected range from the Altitude:

$$\text{Sea Surface Height} = \text{Altitude} - \text{Corrected Range}$$



The sea level anomaly (SLA), also referred to as Residual Sea Surface, is defined here as the sea surface height minus the mean sea surface and minus known geophysical effects, namely tidal and inverse barometer. It is given by:

$$\begin{aligned} \text{Sea Level Anomaly} = & \text{Sea Surface Height} - \text{Mean Sea Surface} \\ & - \text{Solid Earth Tide Height} \\ & - \text{Geocentric Ocean Tide Height} \\ & - \text{Non Equilibrium Long Period} \\ & - \text{Internal Tide Height} \\ & - \text{Pole Tide Height} \\ & - \text{Dynamic Atmospheric Correction} \end{aligned}$$

The SLA contains information about:

- Real changes in ocean topography related to ocean currents
- Dynamic response to atmospheric pressure
- Differences between tides and the tide models
- Differences between the mean sea surface model and the true mean sea surface at the Jason-3 location
- Unmodeled or mismodeled measurement effects (skewness, sea state bias, altimeter errors, tropospheric corrections, ionospheric correction, etc.)
- Orbit errors

There is naturally also random measurement noise. Understanding the first four items as a function of space and time is the purpose of Jason-3.

Altitude :

Orbit altitude (see parameter altitude)

Corrected Range :

See section 4.2.1.

Tide effects (solid earth tide height, geocentric ocean tide height, pole tide height) :

See sections 4.2.2.1 and 5.10.

Dynamic Atmospheric Correction:

Use dac (see also section 5.11).

Mean Sea Surface :

See sections 4.2.2.2 and 5.4.

4.2.2.1. Tide Effects

The total tide effect on the sea surface height is the sum of five values from the (O)(I)GDR:

$$\begin{aligned} \text{Tide Effect} = & \text{Geocentric Ocean Tide} \\ & + \text{Non Equilibrium Long Period} \\ & + \text{Solid Earth Tide} \\ & + \text{Pole Tide} \\ & + \text{Internal Tide} \end{aligned}$$

(See also section 5.10 and subsections)



Geocentric Ocean Tide :

The geocentric ocean tide provided on the (O)(I)GDR is actually the sum of the ocean tide effect and the self-attraction and loading tide effect.

$$\text{Geocentric Ocean Tide} = \text{Ocean Tide} + \text{Load Tide}$$

The (O)(I)GDR provides a choice of two geocentric ocean tide values, `ocean_tide_fes` and `ocean_tide_got`. Each uses a different model for the sum of the ocean tide and loading tide heights for high frequencies (diurnal, semi-diurnal and non-linear tides with higher frequencies), but both include an equilibrium representation of the long-period ocean tides at all long-periods except for the zero frequency (permanent tide) term which is not included. Note that the (O)(I)GDR also explicitly provides the loading tide height from each of the two models that are used to determine the two geocentric ocean tide values, `load_tide_fes`, `load_tide_got`, so the pure ocean tide can be determined by subtracting the load tide value from the geocentric ocean tide value. Obviously, the geocentric ocean tide values and loading tide values should added simultaneously, since the loading tide height would be modeled twice.

Non Equilibrium long-period Tide :

Use `ocean_tide_non_eq`

$$\text{Geocentric Ocean Tide} = \text{Ocean Tide} + \text{Load Tide} + \text{Non Equilibrium Long-Period Tide}$$

Adding the field `tide_neq_lp` to the geocentric ocean tide, allows computing a more complete geocentric ocean tide signal including the dynamic ocean response and the corresponding SAL effect for 6 long period tidal frequencies.

Solid Earth Tide :

Use `solid_earth_tide`

NOTE: Zero frequency (permanent tide) term not included in this parameter.

Pole Tide :

Use `pole_tide`

The tide values all have the same sign/sense in that positive numbers indicate that the surface is farther from the center of the Earth.

Internal Tide :

Use `internal_tide`

The (O)(I)GDR provides one internal tide value, computed from Zaron (2019) model. It models the internal tides surface signatures which remain coherent with the four main barotropic tide frequencies.



4.2.2.2. Geophysical Surface - Mean Sea Surface or Geoid

The geophysical fields Geoid (geoid) - actually geoid undulation, but called simply geoid - and Mean Sea Surface (mean_sea_surface_cnescls and mean_sea_surface_dtu) are distances above the reference ellipsoid, as is the Sea Surface Height. These values are for the location indicated by latitude and longitude. If the values of these fields are needed at a different location within the current frame, along-track interpolation may be done using the high rate (20/second) range and altitude values.

As the geoid is derived from the mean sea surface, the latter is the better-known quantity. The residual surface with respect to the geoid is sometimes called the "dynamic topography" of the ocean surface.

See also discussions of mean sea surface and geoid in sections 5.3 and 5.4.

4.2.3. Mean Sea Surface and Adjustment of the Cross Track Gradient

In order to study sea level changes between two dates, it is necessary to difference sea surface heights from different cycles at the exact same latitude-longitude, so that the not well-known time-invariant geoid cancels out. However, the (O)(I)GDR samples are not given at the same latitude-longitude on different cycles. They are given approximately every 1 sec along the pass (about 6 km, the time difference and distance vary slightly with satellite height above the surface), and the satellite ground track is allowed to drift by ± 1 km. This introduces a problem: on different cycles the satellite will sample a different geoid profile. This effect is the so-called cross-track geoid gradient, and *Brenner and Koblinsky* [1990] estimated it at about 2 cm/km over most of the ocean, larger over continental slopes, reaching 20 cm/km at trenches. Even if the passes repeated exactly, one would have to interpolate along the pass (say, to a fixed set of latitudes) because a 3 km mismatch in along pass position would cause approximately a 6 cm difference in the geoid, which would mistakenly be interpreted as a change in oceanographic conditions.

Both problems are simultaneously solved if the quantity one interpolates along a given pass is the difference

Residual Height - Mean Sea Surface

Then the real geoid changes across the track are automatically accounted for (to the extent the MSS model is close to the true geoid) because the MSS is spatially interpolated to the actual satellite latitude-longitude in the (O)(I)GDR. The residual height term above is the residual sea surface height after applying all the tidal, atmospheric and ionospheric corrections, etc. Otherwise, those need to be interpolated separately.

One possible approach is to interpolate along track to a set of common points, a "reference" track. The reference could be:

- An actual pass with maximum data and/or minimum gaps, or
- A specially constructed fixed track (see below)

The procedure is the following:

- For each common point, find neighboring points in the pass of interest (POI).
- In the POI, interpolate along track to the common point, using longitude as the independent variable, for each quantity of interest - sea surface height (see above), mean sea surface, geoid, tides, etc.
- As stated above, the quantity to compare at each common point is :

$$\Delta\text{SSH} = \text{Interpolated POI SSH} - \text{Interpolated POI MSS}$$

- Other geophysical corrections must be applied to dSSH, depending on the type of investigation



The geoid model in the (O)(I)GDR could substitute the MSS model, but its use will result in reduced accuracy in the interpolation because the resolution of the geoid undulation is lower than that of the MSS.

Desirable features of a fixed reference track include:

- Equal spacing of points (good for FFT)
- Independent variable = (point longitude - pass equator crossing longitude)
- Equator is a point (simplifies calculation)
- Point density similar to original data density

With these specifications, it is possible to make only two fixed tracks, one ascending and one descending, which will serve for all passes. The template pass is then shifted by the equator crossing longitude (global attribute of the product, see 6.3) of each pass. Recall that the equator longitude is from a predicted orbit (not updated during GDR processing). Improved accuracy can be obtained by interpolating in the latitude, longitude values. When one interpolates to the reference track, it is good practice to check that the interpolated latitude from the data records used is close to the latitude on the reference track.

4.2.4. Total Electron Content from Ionosphere Correction

To calculate Ionospheric Total Electron Content, TEC, use the following formula:

$$\text{Ionospheric Total Electron Content} = -\frac{dR * f^2}{40.3}$$

Where :

- Ionospheric Total Electron Content is in electrons/m²
- dR = Ku band ionospheric range correction from the (O)(I)GDR in meters (iono_cor_alt, resp. iono_cor_alt_mle3 for MLE3)
- f = frequency in Hz (13.575 GHz for the Ku band)

Note that the TEC could then be converted to a C band ionosphere range correction using the same formula above, but with the C band frequency of 5.3 GHz.

4.2.5. Range Compression

Each 1Hz frame of the Poseidon-3B Ku (data01/ku/range_ocean, resp. data01/ku/range_ocean_mle3 for MLE3) and C band range measurements (data01/c/range_ocean) are derived from the linear regression of the respective valid 20 Hz range measurements (data_20/ku/range_ocean, resp. data_20/ku/range_ocean_mle3 for MLE3, data_20/ku/range_adaptive for Adaptive and data_20/c/range_ocean).

An iterative outlier detection scheme is adopted in this linear regression and the resulting 20 Hz measurements are identified by setting the corresponding parameter (range_ocean_compression_qual, resp. range_ocean_mle3_compression_qual, range_adaptive_compression_qual) to 1. Measurements not considered as outliers have the parameter set to 0.

The number of valid 20 Hz measurements that are used to derive each of the 1 Hz measurements is provided on the (O)(I)GDRs (ku/range_ocean_numval, resp. ku/range_ocean_mle3_numval for MLE3, resp. ku/range_adaptive_numval for Adaptive, and c/range_ocean_numval), as are the root-mean-square of the differences between the valid 20 Hz measurements and the derived 1 Hz measurement (ku/range_ocean_rms, resp. ku/range_ocean_mle3_rms for MLE3, resp. ku/range_adaptive_rms for Adaptive and ku/range_ocean_rms).



Jason-3 Products Handbook

Iss :2.1 - date : June 21^h , 2021



53

Specialized applications, such as over land, ice, lakes or rivers, may require that the users perform their own compression algorithm on the 20 Hz measurements.



5. Altimetric data

This section presents a short discussion of the main quantities on the (O)(I)GDR.

An excellent overview of the theoretical and practical effects of radar altimetry is the “Satellite Altimetry” Chapter by *Chelton et al* [2001].

5.1. Precise Orbits

CNES has the responsibility for producing the orbit ephemerides for the Jason-3 data products. The Jason-3 OGDRs provide a navigator orbit that has radial accuracies better than 5 cm (RMS), the Jason-3 IGDRs provide a preliminary orbit that has radial accuracies better than 2.5 cm (RMS), while the GDRs provide a precise orbit that has radial accuracies better than 1.5 cm (RMS).

5.2. Altimeter Range

An altimeter operates by sending out a short pulse of radiation and measuring the time required for the pulse to return from the sea surface. This measurement, called the altimeter range, gives the distance between the instrument and the sea surface, provided that the velocity of the propagation of the pulse and the precise arrival time are known. The dual frequency altimeter on Jason-3 performs range measurements at the Ku and C band frequencies (see `ku/range_ocean` and `c/range_ocean`), enabling measurements of the range and the total electron content (see discussion below on ionosphere). While both range measurements are provided on the (I)GDR (see `ku/range_ocean` and `c/range_ocean`), the Ku band range measurement has much higher accuracy than the C band measurement.

The range reported on the Jason-3 (O)(I)GDR has already been corrected for a variety of calibration and instrument effects, including calibration errors, pointing angle errors, center of gravity motion, and terms related to the altimeter acceleration such as Doppler shift and oscillator drift. The sum total of these corrections also appears on the (O)(I)GDR for each of the Ku and C band ranges (see `range_cor_ocean_net_instr`, `range_cor_ocean_mle3_net_instr` and `range_cor_adaptive_net_instr`).

5.3. Geoid

The geoid is an equipotential surface of the Earth's gravity field that is closely associated with the location of the mean sea surface. The reference ellipsoid is a bi-axial ellipsoid of revolution. The center of the ellipsoid is ideally at the center of mass of the Earth although the center is usually placed at the origin of the reference frame in which a satellite orbit is calculated and tracking station positions given. The separation between the geoid and the reference ellipsoid is the geoid undulation (see geoid parameter).

The geoid undulation, over the entire Earth, has a root mean square value of 30.6 m with extreme values of approximately 83 m and -106 m. Although the geoid undulations are primarily long wavelength phenomena, short wavelength changes in the geoid undulation are seen over seamounts, trenches, ridges, etc., in the oceans. The calculation of a high resolution geoid requires high resolution surface gravity data in the region of interest as well as a potential coefficient model that can be used to define the long and medium wavelengths of the Earth's gravitational field. Surface gravity data are generally only available in certain regions of the Earth and spherical harmonic expansions of the Earth's gravitational potential are usually used to define the geoid globally. Currently, such expansions are available to degree 360 and in some cases higher.

For ocean circulation studies, it is important that the long wavelength part of the geoid be accurately determined.



5.4. Mean Sea Surface

A Mean Sea Surface (MSS) represents the position of the ocean surface averaged over an appropriate time period to remove annual, semi-annual, seasonal, and spurious sea surface height signals. A MSS is given as a grid with spacing consistent with the altimeter and other data used in the generation of the grid values. The MSS grid can be useful for data editing purposes, for the calculation of along track and cross track geoid gradients, for the calculation of gridded gravity anomalies, for geophysical studies, for a reference surface to which sea surface height data from different altimeter missions can be reduced, etc. The Jason-3 (O)(I)GDR provides a global MSS model that is generated from multiple satellite altimetry missions.

Longer time spans of data that become available in the future, along with improved data handling techniques will improve the current MSS models. Care must be given to the retention of high frequency signal and the reduction of high frequency noise.

5.5. Mean Dynamic Topography

A Mean Dynamic Topography (MDT) represents the Mean Sea Surface referenced to a geoid and corrected from geophysical effects. A MDT is given as a grid with spacing consistent with the altimeter and other data used in the generation of the grid values. The MDT provides the absolute reference surface for the ocean circulation. The Jason-3 (O)(I)GDR provides a global MDT model that is a combined product recovering several years based on GRACE mission, altimetry and in situ data (hydrologic and drifters data).

5.6. Geophysical Corrections

The atmosphere and ionosphere slow the velocity of radio pulses at a rate proportional to the total mass of the atmosphere, the mass of water vapor in the atmosphere, and the number of free electrons in the ionosphere. In addition, radio pulses do not reflect from the mean sea level but from a level that depends on wave height and wind speed. The errors due to these processes cannot be ignored and must be removed. Discussions of these effects are given in *Chelton et al.* [2001].

5.6.1. Troposphere (Dry and Wet)

The propagation velocity of a radio pulse is slowed by the "dry" gases and the quantity of water vapor in the Earth's troposphere. The "dry" gas contribution is nearly constant and produces height errors of approximately -2.3 m. The water vapor in the troposphere is quite variable and unpredictable and produces a height calculation error of -6 cm to -40 cm. However, these effects can be measured or modeled as discussed below.

5.6.1.1. Dry Troposphere

The gases in the troposphere contribute to the index of refraction. In detail, the refractive index depends on pressure and temperature. When hydrostatic equilibrium and the ideal gas law are assumed, the vertically integrated range delay is a function only of the surface pressure, see *Chelton et al.* [2001]. The dry meteorological tropospheric range correction is principally equal to the surface pressure multiplied by -2.277mm/mbar, with a small adjustment also necessary to reflect a small latitude dependence see Saastamoinen [1972] .

$$\text{model_dry_tropo_cor_measurement_altitude} = -2.277 * P_{\text{atm}} * [1 + 0.0026 * \cos(2 * \text{phi})]$$

where P_{atm} is surface atmospheric pressure at Digital Elevation Model (DEM) in mbar, phi is latitude, and $\text{model_dry_tropo_cor_measurement_altitude}$ is the dry troposphere correction in mm at DEM altitude.



$$\text{model_dry_tropo_cor_zero_altitude} = -2.277 * P_{\text{atm}} * [1 + 0.0026 * \cos(2 * \text{phi})]$$

where P_{atm} is surface atmospheric pressure at Mean Sea Level (MSL) in mbar, phi is latitude, and $\text{model_dry_tropo_cor_zero_altitude}$ is the dry troposphere correction in mm at MSL altitude.

Since GDR-F, at GDR level, a new approach is used for the model dry tropospheric delay (see $\text{model_dry_tropo_cor_measurement_altitude}$) : it is estimated directly at measurement altitude from altimeter range integrating Analysed 3D ECMWF humidity, temperature and cloud liquid water content.

There is no straightforward way of measuring the nadir surface pressure from a satellite, so it is determined from the European Center for Medium Range Weather Forecasting (ECMWF) numerical weather prediction model. The uncertainty on the ECMWF atmospheric pressure products is somewhat dependent on location. Typical errors vary from 1 mbar in the northern Atlantic Ocean to a few mbars in the southern Pacific Ocean. A 1-mbar error in pressure translates into a 2.3 mm error in the dry tropospheric correction.

The use of parameters estimated at DEM or measurement altitude for model dry and wet tropospheric corrections are recommended for hydrological application [Valladeau *et al.*, 2015]

5.6.1.2. Wet Troposphere

The amount of water vapor present along the path length contributes to the index of refraction of the Earth's atmosphere. Its contribution to the delay of the radio pulse, the wet tropospheric delay, can be estimated by measuring the atmospheric brightness near the water vapor line at 22.2356 GHz and providing suitable removal of the background. The Jason-3 Microwave Radiometer (AMR) measures the brightness temperatures in the nadir path at 18.7, 23.8 and 34.0 GHz: the water vapor signal is sensed by the 23.8 GHz channel, while the 18.7 GHz channel removes the surface emission (wind speed influence), and the 34 GHz channel removes other atmospheric contributions (cloud cover influence) [Keihm *et al.*, 1995].

Measurements are combined to obtain the path delay in the satellite range measurement due to the water vapor content (see rad_wet_tropo_cor parameter).

The uncertainty is less than 1.2 cm RMS [e.g. Cruz Pol *et al.*, 1998 and Ruf *et al.*, 1994]. Since GDR-D product version, an improved near land wet path delay algorithm is applied to improve the performance up to the coast. The algorithm error when applied to the AMR is estimated to be less than 0.8 cm up to 15 km from land, less than 1.0 cm within 10 km from land, less than 1.2 cm within 5 km from land and less than 1.5 cm up to the coastline. This is estimated from detailed simulations and validated by comparisons with measured AMR data [Brown, 2009]. The radiometer surface type (see $\text{rad_surface_type_flag}$ parameter) indicates the quality of this wet tropospheric correction.

The ECMWF numerical weather prediction model provides also a value for the wet tropospheric delay estimated at DEM altitude. An interpolated value from this model is included in the OGDR and IGDR level, as a backup to the measurement from the AMR (see $\text{model_wet_tropo_cor_measurement_altitude}$). This backup will prove useful when sun glint, land contamination, or anomalous sensor behavior makes the AMR measurement of the wet tropospheric delay unusable. The same value is also provided in the (O)(I)GDR (see $\text{model_wet_tropo_cor_zero_altitude}$).

An interpolation quality flag is provided on the (O)(I)GDR to indicate the quality of this interpolation (see $\text{meteo_zero_altitude_interp_qual}$).

Since GDR-F, at GDR level, a new approach is used for the model wet tropospheric delay (see $\text{model_wet_tropo_cor_measurement_altitude}$) : it is estimated directly at measurement altitude from altimeter range integrating Analysed 3D ECMWF humidity, temperature and cloud liquid water content.



5.6.2. Atmospheric Attenuation

See sig0_cor_atm

The radiometer solution is retrieved with the same approach detailed in the previous section.

When the radiometer is not available, a model solution is given. It is established from ECMWF analysis based on the equations provided by Keihm, 1995 for OGDR and IGDR, and Lillibridge et al., 2014 for GDR. In this later, pressure, temperature, humidity and cloud liquid water content ECMWF profiles are combined through polynomial relation to compute the model atmospheric attenuation at the measurement altitude.

A flag indicates whether the radiometer solution or the model solution is provided in sig0_cor_atm (see sig0_cor_atm_source)

5.6.3. Ionosphere

At the frequencies used by the Poseidon-3B altimeter, the propagation velocity of a radio pulse is slowed by an amount proportional to the density of free electrons of the Earth's ionosphere, also known as the total electron content (TEC). The retardation of velocity is inversely proportional to frequency squared. For instance, it causes the altimeter to slightly over-estimate the range to the sea surface by typically 0.2 to 20 cm at 13.6 GHz. The amount varies from day to night (there are fewer free electrons at night), from summer to winter, and as a function of the solar cycle (there are fewer during solar minimum.) (For discussions on this correction, see *Chelton et al.* [2001], *Imel* [1994], and *Callahan* [1984].

Because this effect is dispersive, measuring the range at two frequencies allows it to be estimated. Under typical ocean conditions of 2-meter significant wave height, the Ku band ionospheric range correction determined from the dual frequency measurements from the altimeter is expected to have an accuracy of ± 0.5 cm (see iono_cor_alt parameter).

To reduce the noise a smoothed solution, derived from [*Imel*, 1994], is provided in the product (see iono_cor_alt_filtered parameter).

A backup ionospheric correction solution, derived from Global Ionosphere Maps (GIM), is provided in the (I)GDR products (see iono_cor_gim parameter). It may be used over non ocean surfaces (ice, land, etc.).

5.6.4. Ocean Waves (sea state bias)

Unlike the preceding effects, sea-state effects are an intrinsic property of the large footprint radar measurements. The surface scattering elements do not contribute equally to the radar return; troughs of waves tend to reflect altimeter pulses better than do crests. Thus the centroid of the mean reflecting surface is shifted away from mean sea level towards the troughs of the waves. The shift, referred to as the electromagnetic (EM) bias, causes the altimeter to overestimate the range (see *Rodriguez et al.*, [1992]). In addition, a skewness bias also exists from the assumption in the onboard algorithms that the probability density function of heights is symmetric, while in reality it is skewed. Finally, there is a tracker/processing bias, which is a combination of instrumental and processing choices effect. The sum of EM bias, skewness bias, and tracker/processing bias is called 'sea state bias' (see ku/ and c/ sea_state_bias parameters).

The accuracy of the sea state bias models remains limited and continues to be a topic of research. The current most accurate estimates are obtained by using empirical models derived from analyses of the altimeter data themselves. The sea state bias is computed from a bilinear interpolation of a table of sea state biases versus significant wave height and wind speed, based on empirical fits (Labroue [2004]). For a typical significant wave height (SWH) of 2 meters, the sea state bias is about 10 cm, and the error (bias) in the sea state bias correction is approximately 1-2 cm. The



noise of the sea state bias estimates depends mainly on the noise on the significant wave height estimates.

The 3D version consists in a table with a third input, the mean wave period provided by a wave model to better describe the local wave conditions and thus improves the sea state bias estimates [Tran et al, 2010].

5.7. Rain Flag

Liquid water along the pulse's path reduces the energy returned to the altimeter, mainly at Ku band. In heavy rain, there are competing effects from attenuation and surface changes. The small-scale nature of rain cells tends to produce rapid changes in the strength of the echo as the altimeter crosses rain cells. Both effects degrade the performance of the altimeter. Data contaminated by rain are rare (most are located in the west equatorial pacific), flagged and should be ignored (see `rain_flag` parameter).

The rain flag on the Jason-3 (O)(I)GDR is set if integrated liquid water content measured by the AMR is larger than a specified threshold, AND if the difference between the expected Ku-band backscatter coefficient (estimated from the C-band backscatter coefficient which is much less affected by rain) and the measured Ku-band backscatter coefficient, is larger than either a specified threshold or a specified multiple of the uncertainty in the expected Ku-band backscatter coefficient (see `rain_flag` parameter) [Tournadre and Morland, 1998]. Ku band backscatter coefficient used for the rain flag determination is issued from MLE3 retracking (`ku/sig0_ocean_mle3` and `c/sig0_ocean`).

A radiometer derived rain flag (see `rad_rain_flag` parameter) is also computed through a comparison of the 18.7 GHz brightness temperature and the cloud liquid water observed by the AMR to specific thresholds. Rain is very absorptive in the microwave, and, over ocean, increases significantly and proportional to the rain rate the brightness temperature and the cloud liquid water observed by the AMR. Over the ocean, only rain will cause the 18.7 GHz brightness temperature to rise above ~200 K.

5.8. Ice Flag

The range measurement from the altimeter is likely to have larger errors when the pulse is reflected off ice surfaces. The ice surface is not at sea level, but at some unknown distance above it. For this reason the JASON-3 (O)(I)GDR provides an ice flag (see `ice_flag` parameter) to indicate when the data point is likely to be over ice.

The ice flag is set if the absolute value of the difference between the model wet tropospheric correction and the dual frequency wet tropospheric correction retrieved from 23.8 GHz and 34.0 GHz brightness temperatures exceeds a specified threshold, OR if the number of valid 20-Hz altimeter range of the processed measurement is smaller than a specified threshold. If the corresponding computations cannot be performed, then the ice flag is set if a climatological map predicts ice at the given location and if the wind speed derived from the altimeter measurement is less than 1 m /s, i.e., the backscatter is larger than normally expected from the ocean.

A radiometer derived sea ice flag (see `rad_sea_ice_flag`) is also computed through the comparison between the AMR 34.0 GHz channels and 18.7 GHz brightness temperatures. Sea ice has an emissivity near 1 in the microwave and has a small frequency dependence. This contrasts from the open ocean brightness temperature. The difference between the AMR 34.0 GHz channels and 18.7 GHz channels is near 20-30 K in the open ocean, but generally less than 10K when sea ice is present. As the difference is also small for land, sea ice presence is assessed using the radiometer surface type flag.



5.9. Waveform Classification

In open ocean, the shape of the altimetric echoes follows the Brown model. It is a well-known and relatively constant shape. But when the overflown surface is non-homogeneous, the waveform amplitude and shape are modified. The first step of our study is to analyze individual measurements at different locations of interest.

For defining the new class list, many waveforms have been observed on different surfaces: open ocean, coastal areas, hydrology, sea ice and land ice. Waveforms are randomly picked over all the different surfaces. From all these areas, typical echo shapes have been defined based on their occurrence in the resulting echo database

The resulting list of classes must correspond to all representative shapes that are encountered on the different surfaces. It is important to define a class for each echo shape of interest but also for all other waveforms numerous enough to impact the classifier. Even if they do not provide useful information for the user, their identification as a dedicated class number prevents the algorithm from misclassifying them as shapes of interest. Knowing all these constraints, the list of classes defined for the Jason-3 waveform classification is detailed hereafter.

0	1	2	3	4	5	6	7
8	9	10	11	12	13	15	18
	<i>Trash waveforms</i>						

Table 19 : List of classes defined for Jason-3 waveforms

- **Class 1:** Brownian echoes, mainly found in open ocean
- **Class 2:** peaky echoes, mainly encountered over narrow rivers, small lakes (smaller than the altimeter footprint) and water leads in sea ice regions
- **Class 3:** several peaks, corresponds to multiple reflection in the footprint, encountered over land or heterogeneous areas
- **Class 4:** strong peak with a very low trailing edge, corresponds to high reflective surfaces, often encountered on sea ice, most of the time over First Year Ice (FYI)
- **Class 5:** Brownian shape with a peak on the trailing edge, mainly found in coastal areas where the altimeter is close to the coast and a “bright point” is present in the footprint (but not at nadir)
- **Class 6:** Brownian shape with a peak on the leading edge or Brownian shape with a sharp trailing edge. Can be encountered over sea ice.
- **Class 7:** Brownian shape with a flat or increasing trailing edge. Can be found in rain cells or over land ice (it can also be a sign of a platform mispointing even if Jason-3 have good pointing performances).
- **Class 8:** peaky echo shifted at the end of the analysis window, mainly found on hydrology and land
- **Class 9:** trash echoes
- **Class 10:** Brownian shape with a high thermal noise level mainly found on land, land ice and sometimes on very heavy rain event



- Class 11: Double leading edge, can be encountered over land
- Class 12: shifted Brownian, can be found over land ice and hydrology (big lake with a non-optimal tracker command)
- Class 13: Brownian shape with a noisy leading edge
- Class 15: linear rise, can be found over land
- Class 18: linear decrease, can be found over land

The method used [Poisson 2020] is a neural network with one hidden layer of 23 neurons connecting 9 inputs parameters and 15 outputs classes (Inputs-Hidden-Outputs: 9-23-15). The neurons, within the hidden layer perform the same function. They simply calculate the weighted sum of inputs and weights, add the bias and execute an activation function (sigmoid). This final set of parameters for the neural network was analyzed and optimized in order to have the best performances of the network in term of prediction.

5.10. Tides

Tides are a significant contributor to the observed sea surface height [LeProvost, 2001]. While they are of interest in themselves, they have more variation than all other time-varying ocean signals. Since they are highly predictable, they are removed from the data in order to study ocean circulation. The T/P orbit was specifically selected (inclination and altitude) so that diurnal and semidiurnal tides would not be aliased to low frequencies.

There are several contributions to the tidal effect: the ocean tide, the load tide, the solid earth tide, the pole tide and the internal tide. The ocean tide, load tide, solid earth tide and internal tide are all related to luni-solar forcing of the earth, either directly as is the case of the ocean and solid earth tides, or indirectly as is the case with the load tide since it is forced by the ocean tide. The internal tide is forced by the ocean tide flow over sharp bottom topography. The pole tide is due to variations in the earth's rotation axis and is unrelated to luni-solar forcing.

Jason-3 (O)(I)GDRs do not explicitly provide values for the pure ocean tide, but instead provide values for a quantity referred to as the geocentric ocean tide, which is the sum total of the ocean tide and the load tide. Values of the load tide that were used to compute the geocentric ocean tide are also explicitly provided, so the pure ocean tide can be determined by subtracting the load tide value from the geocentric ocean tide value. Note that the permanent tide is not included in either the geocentric ocean tide or solid earth tide corrections that are provided on the Jason-3 (O)(I)GDRs.

5.10.1. Geocentric Ocean Tide

As mentioned above, the geocentric ocean tide refers to the sum of the ocean tide and the load tide. The Jason-3 (O)(I)GDR provides two choices for the geocentric ocean tide, `ocean_tide_fes` and `ocean_tide_got`: each of them is computed as the sum of the ocean and load tides as predicted by a particular model for high frequencies (diurnal, semi-diurnal and non-linear tides with higher frequencies), and an equilibrium representation of the long-period ocean tides at all long-periods except for the zero frequency (constant) term which is not included. The two load tide values provided in the GDR, `load_tide_fes` and `load_tide_got`, provide the respective load tide values that were used to compute `ocean_tide_fes` and `ocean_tide_got`. As the ocean tide is set to zero on lakes and enclosed-seas, parameters `ocean_tide_fes` and `ocean_tide_got` are equal to the load tide value on these surfaces.

5.10.2. Long period Ocean Tide

The long-period ocean tides are a subject of continuing investigation. To first order, they can be approximated by an equilibrium representation. However, the true long-period ocean tide response



is thought to have departures from an equilibrium response that increase with decreasing period. The two principal long-period ocean tide components, Mf and Mm, with fortnightly and monthly periods respectively, are known to have departures from an equilibrium response with magnitudes less than 1-2 cm.

The Jason-3 (O)(I)GDR explicitly provides a value for an equilibrium representation of the long-period ocean tide that includes all long-period tidal components excluding the permanent tide (zero frequency) component (see parameter `ocean_tide_eq`). Note that both geocentric ocean tide values on the (O)(I)GDR (`ocean_tide_fes` and `ocean_tide_got`) already include the equilibrium long-period ocean tide and should therefore not be used simultaneously.

The Jason-3 (O)(I)GDR also provides a parameter for a non-equilibrium representation of the long-period ocean tides (see parameter `ocean_tide_non_eq`). This parameter is provided as a correction to the equilibrium long-period ocean tide model so that the total non-equilibrium long period ocean tide is formed as a sum of `ocean_tide_eq` and `ocean_tide_non_eq`. The non-equilibrium long-period ocean tide provided in the Jason-3 (O)(I)GDR comes from FES2014b tide model, but the parameter `ocean_tide_non_eq` can be used either with the `ocean_tide_fes` or the `ocean_tide_got`.

FES2014b model provides a dynamic solution for 6 long-period tidal frequencies: Mf, Mm, MSqm, Mtm, Sa, Ssa.

Parameter `ocean_tide_eq` is set to zero on lake and enclosed-seas, and the ocean tide part of the parameter `ocean_tide_non_eq` is also set to zero on these surfaces.

5.10.3. Solid Earth Tide

The solid Earth responds to external gravitational forces similarly to the oceans. The response of the Earth is fast enough that it can be considered to be in equilibrium with the tide generating forces. Then, the surface is parallel with the equipotential surface, and the tide height is proportional to the potential. The two proportionality constants are the so-called Love numbers. It should be noted that the Love numbers are largely frequency independent, an exception occurs near a frequency corresponding to the K1 tide constituents due to a resonance in the liquid core [Wahr, 1985 and Stacey, 1977].

The Jason-3 (O)(I)GDR computes the solid earth tide, or body tide, as a purely radial elastic response of the solid Earth to the tidal potential (see parameter `solid_earth_tide`.) The adopted tidal potential is the *Cartwright and Tayler* [1971] and *Cartwright and Edden* [1973] tidal potential extrapolated to the 2000 era, and includes degree 2 and 3 coefficients of the tidal potential. The permanent tide (zero frequency) term is excluded from the tidal potential that is used to compute the solid earth tide parameter for the Jason-3 (O)(I)GDR. The elastic response is modeled using frequency independent Love numbers. The effects of the resonance in the core are accounted for by scaling the tide potential amplitude of the K1 tidal coefficient and some neighboring nodal terms by an appropriate scale factor.

5.10.4. Pole Tide

The pole tide is a tide-like motion of the ocean surface that is a response of both the solid Earth and the oceans to the centrifugal potential that is generated by small perturbations to the Earth's rotation axis. These perturbations primarily occur at periods of 433 days (called the Chandler wobble) and annual. These periods are long enough for the pole tide displacement to be considered to be in equilibrium with the forcing centrifugal potential. The Jason-3 (O)(I)GDR provides a single field for the radial geocentric pole tide displacement of the ocean surface (see `pole_tide` parameter), and includes the radial pole tide displacement of the solid Earth and the oceans.

The pole tide is easily computed as described in [Wahr, 1985] and [Desai et al, 2017]. This new algorithm accounts for self-gravitation, loading, conservation of mass, and geocenter motion (spatial dependence). Over the oceans the pole tide includes the response of the solid earth, ocean, and loading effect; over land it includes only the impact on the solid earth and loading.



The mean pole variation model includes a bias AND a drift (temporal dependence), and the computed pole tide does NOT include the effects of the Earth's displacement response to that mean pole (drift).

Modeling the pole tide requires knowledge of proportionality constants, the so-called Love numbers, and a time series of perturbations to the Earth's rotation axis, a quantity that is now measured routinely with space techniques. Note that the pole tide on the IGDR and GDR may differ, since the pole tide on the GDR is computed with a more accurate time series of the Earth's rotation axis.

5.10.5. Internal Tide

Internal tides are baroclinic tides generated by the arrival of a barotropic tide flow on an underwater sharp topography pattern (seamount or shelfbreak region); they can reach amplitudes of several 10th of meters at the thermocline level and they have a signature of several cm at the surface with wavelengths about 50-250 km for the first mode and shorter wavelengths for higher modes.

To reach higher accuracy ocean signals using the Jason-3 (O)(I)GDR, we need to be able to separate all tides signals, including the small scale internal tides surface signatures, from other oceanic signals.

The global ocean tide models described in previous sections are barotropic tide models, so by essence they do not correct from the internal tides signature at the surface.

The Jason-3 (O)(I)GDR provides a value for the internal tide surface signature, taking into account the M2,S2,K1,O1 tidal frequencies from Zaron model [Zaron, 2019].

See parameter `internal_tide`.

5.11. Ocean response to atmospheric forcing

5.11.1. Inverted Barometer Correction

As atmospheric pressure increases and decreases, the sea surface tends to respond hydrostatically, falling or rising respectively. Generally, a 1-mbar increase in atmospheric pressure depresses the sea surface by about 1 cm. This effect is referred to as the inverse barometer (IB) effect.

The instantaneous IB effect on sea surface height in millimeters (see parameter `inv_bar_cor`) is computed from the surface atmospheric pressure, P_{atm} in mbar:

$$\text{inv_bar_cor} = -9.948 * (P_{atm} - P)$$

where P is the time varying mean of the global surface atmospheric pressure over the oceans.

The scale factor 9.948 is based on the empirical value [Wunsch, 1972] of the IB response at mid latitudes. Some researchers use other values. Note that the surface atmospheric pressure is also proportional to the dry tropospheric correction, and so the parameter `inv_bar_cor` approximately changes by 4 to 5 mm as `model_dry_tropo_cor_zero_altitude` changes by 1 mm (assuming a constant mean global surface pressure). The uncertainty of the ECMWF atmospheric pressure products is somewhat dependent on location. Typical errors vary from 1 mbar in the northern Atlantic Ocean to a few mbars in the southern Pacific Ocean. A 1-mbar error in pressure translates into a 10 mm error in the computation of the IB effect.

Note that the time varying mean global pressure over the oceans, P , during the first eight years of the T/P mission had a mean value of approximately 1010.9 mbar, with an annual variation around this mean of approximately 0.6 mbar. However, the T/P data products provided a static inverse barometer correction referenced to a constant mean pressure of 1013.3 mbar.



$$IB(T/P) = -9.948 * (P_{atm} - 1013.3)$$

Sea surface heights that are generated after applying an inverse barometer correction referenced to a mean pressure of 1013.3 mbar are therefore approximately $-9.948 * (1010.9 - 1013.3) = 23.9$ mm lower than those that are generated after applying an inverse barometer correction referenced to a time varying global mean pressure, and the difference between the two sea surface heights has an annual variation of approximately $9.948 * 0.6 = 6$ mm.

5.11.2. Dynamic Atmospheric Correction

The Dynamic Atmospheric Correction (DAC) allows taking into account the dynamic response of the ocean to atmospheric forcing for high frequencies, and it can be used instead of the Inverted Barometer correction (`inv_bar_cor`). This new field `dac` provided in the Jason-3 (O)(I)GDR replaces the use of the sum of the formerly `hf_fluctuations_corr` + `inv_bar_corr`.

The ocean response to wind and pressure is mostly dynamic and is significantly energetic at short periods so that the static IB correction is not sufficient; several models approaches have been developed and showed that a barotropic model allows a good representation of this variability (Ponte 1991, Stammer et al. 1999, Mathers 2000, Tierney et al. 2000, Carrere 2003, Vinogradova and Ponte 2008).

The DAC is composed from the high frequencies of the barotropic ocean model MOG2D, forced by ECMWF operational wind and pressure fields and the low frequencies of the IB (Carrere and Lyard, 2003). The cut-off frequency is 20 days and corresponds to the Nyquist frequency of the reference TP/Jason altimeters which have a 10 days cycle. DAC is therefore capable of removing almost all the high-frequency dynamic signal forced by the atmosphere (pressure and wind) and aliased in the altimetric measurement, except the errors and uncertainties of the model.

Notice that a slightly different `dac` is provided for each (O)(I)GDR product, due to the use of a different centering of the filtering window and different atmospheric forcings:

- GDR : use of ECMWF operational analysis and an optimal filtering using a full and centered filtering window;
- IGDR: use of ECMWF operational analysis and a filtering window decentered in time but using model forecasts in the future
- OGDR: use of ECMWF operational forecasts and a filtering window decentered in time but using model forecasts in the future

5.12. Sigma 0

The backscatter coefficients, `sigma0_Ku` and `C` values (see parameters `ku/sig0_ocean` and `c/sig0_ocean`), reported on the (O)(I)GDR are corrected for atmospheric attenuation using `ku/sig0_cor_atm` and `c/sig0_cor_atm`.

Note that "nominal" `sigma0` values are recorded on the Jason-3 data products. For the altimeter wind retrieval, a bias is applied to the provided `sigma` in order to get a 1-year period wind speed distribution form similar to the one observed by ERA5 model.

5.13. Wind Speed

The model functions developed to date for altimeter wind speed have all been purely empirical. A wind speed is calculated through a mathematical relationship with the Ku-band backscatter coefficient and the significant wave height (see `wind_speed_alt`) using the Gourrion approach [Gourrion et al, 2002] and Collard's model computed from Jason-1 data [Collard, 2005].

A calibration bias is applied on Jason-3 Ku-band backscatter coefficient (cf. 5.12) This bias was updated for Jason-3 GDR-F : +0.06dB for MLE4 , +0.109 dB for MLE3, and +0,08 for Adaptive.



The wind speed model function is evaluated for 10 meter above the sea surface, and is considered to be accurate to 2 m/s.

A radiometer derived wind speed is also computed through an empirical relationship to brightness temperatures measured by the AMR [Keihm *et al.*, 1995] (see `wind_speed_rad`). The coefficients of this relationship have been determined from the regression of island radiosonde data computations combined with seasonal and latitude dependent wind speed statistics.

Finally, a 10-meter (above surface) wind vector (in east-west and north-south directions) is also provided on the Jason-3 (O)(I)GDR (see parameters `wind_speed_mod_u` and `wind_speed_mod_v`). This wind speed vector is determined from an interpolation of the ECMWF model. The best accuracy for the wind vector varies from about 2 m/s in magnitude and 20 degrees in direction in the northern Atlantic Ocean, to more than 5 m/s and 40 degrees in the southern Pacific Ocean.

5.14. Bathymetry Information

The Jason-3 (O)(I)GDR provides a parameter bathymetry that gives the ocean depth or land elevation of the data point. Ocean depths have negative values, and land elevations have positive values. This parameter is given to allow users to make their own "cut" for ocean depth.



6. Data description

6.1. (O)(I)GDR content

The main characteristics of (O)(I)GDR products are summarized in the following table.

Features	OGDR	IGDR	GDR
Primary Goal	To provide wind/wave data to meteorological users. Also designed to provide altimeter range, environmental and geophysical corrections together with a real-time orbit in order to make NRT SSHA available to ocean users	To provide sea surface height data to operational oceanography users (with a more accurate orbit and additional environmental / geophysical corrections w.r.t. OGDR)	To fulfill the project science objectives (TP4-J0-STB-44-CNES AD 2)
Content	Geophysical level 2 product (Poseidon-3B/AMR), including waveforms retracking		
	+ available environmental and geophysical corrections	+ all the environmental and geophysical corrections (preliminary for some of them)	+ all the environmental and geophysical corrections (precise)
Orbit	5 cm DORIS navigator	2.5 cm MOE (processed DORIS + GPS data)	1.5 cm POE (processed DORIS and/or GPS and/or laser data)
Delivery delay (after data acquisition)	Near-Real Time	Off-Line	Off-Line
	3-5 hours	1 calendar day	90 days
Validation	Not fully validated (elementary and automatic controls only)		Fully validated (in depth validation performed on a cycle basis before delivery)
Validation by Experts	No		Yes (NASA/JPL and CNES/SALP)
Structure	Segment (see 0)	Pole to pole pass	
Ground Processing Centre	NOAA and EUMETSAT	CNES	

Table 20 : Main characteristics of (O)(I)GDR products

The differences between Auxiliary Data used for OGDR, IGDR and GDR products is given in section 1.1. The main fields recomputed for GDR with respect to IGDR are the following:

- Due to the update of orbit data:
 - Latitude (“latitude”)
 - Longitude (“longitude”)
 - Altitude (“altitude”, “orb_state_rest_flag”)
 - Orbital altitude rate (“altitude_rate”)
 - Doppler correction (“range_cor_doppler”)



Sum of the instrumental corrections (“range_cor_ocean_net_instr”)

Corrected ground retracked altimeter ranges (“range_ocean”, “range_ocean_mle3”, “range_adaptive”)

Ionospheric correction (“iono_cor_alt”, “iono_cor_gim”)

- Due to the update of platform data:

Distance antenna-COG correction (“range_cor_cog”)

Sum of the instrumental corrections (“range_cor_ocean_net_instr”)

Corrected ground retracked altimeter ranges (“range_ocean”, “range_ocean_mle3”)

Altimeter ionospheric correction (“iono_cor_alt”)

- Due to the update of pole locations:

Pole tide height (“pole_tide”)

- Due to the update of dac data:

High frequency dealiasing correction (“dac”)

- Due to the update of AMR calibration coefficients:

All the AMR-derived parameters, and mainly as far as altimeter parameters are concerned:

Radiometer wet tropospheric correction (“rad_wet_tropo_cor”)

Atmospheric attenuation (“sig0_cor_atm”)

Backscatter coefficient (“sig0_ocean”)

Altimeter wind speed (“wind_speed_alt”)

Radiometer wind speed (“wind_speed_rad”)

Sea State Bias (“sea_state_bias”)

Rain flag (“rain_flag”)

Radiometer rain flag (“rad_rain_flag”)

Ice flag (“ice_flag”)

Radiometer sea ice flag (“rad_sea_ice_flag”)

6.2. Datasets

Accounting for Jason-2 heritage, products are split into three data sets:

- “SSHA” data set : One file close to Jason-2 SSHA, limited to 1Hz sampling values
- “GDR” data set : One file close to Jason-2 GDR, containing 1Hz and 20Hz values
- “SGDR” data set : One file close to Jason-2 SGDR, containing 1Hz, 20hz and waveforms values

The following figure shows the data sets available for each kind of product.

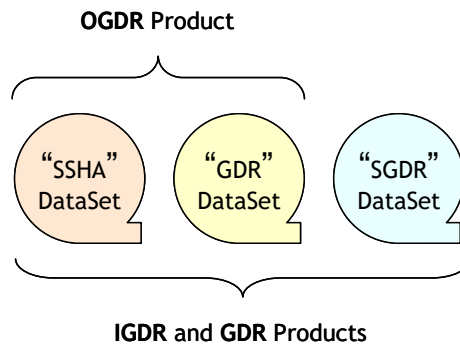


Figure 14 : Data set availability per product

OGDR products are also available in BUFR-formatted dataset for distribution via the World Meteorological Organization (WMO) Global Tele-communication System (GTS).

6.3. Product Description

The [netCDF](#) data format has been chosen to store the different data sets (one file per data set). This format is extremely flexible, self describing and has been adopted as a de-facto standard for many operational oceanography systems. What's more, the files follow the Climate and Forecast NetCDF conventions CF-1.7 because these conventions provide a practical standard for storing.

A netCDF file contains **dimensions**, **variables**, **groups**, and **attributes**, which all have both a name by which they are identified. These components can be used together to capture the meaning of data and relations among data fields in an array-oriented data set.

Full Product description (format, global attributes, groups, dimensions, variables names and their attributes) is provided in [DR9]

6.4. Software

This section lists some software that may be used to browse and use data from SSHA, GDR and SGDR data sets.

6.4.1. Software provided with netCDF : "ncdump"

« ncdump » converts netCDF files to ASCII form (CDL)

See <https://www.unidata.ucar.edu/software/netcdf/workshops/2011/utilities/index.html>

The main options are the following :

- h Show only the header information in the output, that is the declarations of dimensions, variables, and attributes but no data values for any variables
- c Show the values of coordinate variables (variables that are also dimensions) as well as the declarations of all dimensions, variables, and attribute values
- v *var1*,...,*varn* The output will include data values for the specified variables, in addition to the declarations of all dimensions, variables, and attributes
- x *var1*,...,*varn* Output XML (NcML) instead of CDL. The NcML does not include data values



6.4.2. Additional general software

6.4.2.1. ncbrowse

“ncBrowse” is a Java application that provides flexible, interactive graphical displays of data and attributes from a wide range of netCDF data file conventions.

See <http://www.pmel.noaa.gov/epic/java/ncBrowse/>

6.4.2.2. netCDF Operator (NCO)

The netCDF Operators, or “NCO”, are a suite of programs known as **operators**. Each operator is a standalone, command line program which is executed at the UNIX shell-level, like, e.g., `ls` or `mkdir`. The operators take netCDF files as input, then perform a set of operations (e.g., deriving new data, averaging, hyperslabbing, or metadata manipulation) and produce a netCDF file as output. The operators are primarily designed to aid manipulation and analysis of gridded scientific data. The single command style of NCO allows users to manipulate and analyze files interactively and with simple scripts, avoiding the overhead (and some of the power) of a higher level programming environment.

See <http://nco.sourceforge.net/>

6.4.3. Additional specific software: “BRAT”

The “Basic Radar Altimetry Toolbox” is a collection of tools and tutorial documents designed to facilitate the use of radar altimetry data. It is able to read most distributed radar altimetry data from all the satellites, to do some processing, data editing and statistic over them, and to visualise the results. The Basic Radar Altimetry Toolbox is able to read ERS-1 and 2, TOPEX/Poseidon, GEOSAT Follow-on, Jason-1, ENVISAT, OSTM/Jason-2, Jason-3 and CRYOSAT missions altimetry data from official data centres (ESA, NASA/JPL, CNES/AVISO, NOAA), and this for different processing levels, from level 1B (Sensor Geophysical Data Record) to level 3/4 (gridded merged data).

See http://www.altimetry.info/html/data/toolbox_en.html

6.5. OGDR BUFR product

The Global Telecommunications System (GTS) is the coordinated global system of telecommunication facilities and provides rapid collection, exchange and distribution of observations and processed information within the framework of the World Weather Watch. It is implemented and operated by National Meteorological Services of the World Meteorological Organisation (WMO) members and also by a few international organizations (ECMWF, EUMETSAT). The GTS consists of an integrated network of point-to-point circuits, and multi-point circuits which interconnect meteorological telecommunication centres.

Jason-3 BUFR products are designed primarily for dissemination via the GTS and they consequently follow the format conventions defined by the WMO for all data disseminated on the GTS. The WMO FM-94 BUFR (Binary Universal Form for the Representation of Meteorological data), is a binary code designed to represent, employing a continuous binary stream, any meteorological data. It has been designed to achieve efficient exchange and storage of meteorological and oceanographic data. It is self defining, table driven and a very flexible data representation system, especially for big volumes of data.

The following table summarizes how to identify Jason-3 OGDR data in BUFR format on the GTS.

Product	Bulletin header	Originating station	Descriptor sequence
---------	-----------------	---------------------	---------------------



Jason-3 Products Handbook

Iss :2.1 - date : June 21^h , 2021



69

OGDR generated at NOAA	ISZX01	KNES	3-40-010
OGDR generated at EUMETSAT	ISZX01	EUMS	3-40-010
OGDR generated at CNES	ISZX01	LFPW	3-40-010

You will find more details on the BUFR format and the latest tables, on the WMO page:

<https://www.wmo.int/pages/prog/www/WDM/Guides/Guide-binary-1A.html>

Finally, note that ECMWF offers a comprehensive introduction to understanding BUFR format and provides various well documented encoding/decoding tools. All this can be accessed on this page:

<https://www.ecmwf.int/en/learning/training/eccodes-grib-and-bufr-data-decoding-and-encoding-software>



Annexe A - References

- Benada, J. R., 1997, "PO.DAAC Merged GDR (TOPEX/POSEIDON) Generation B User's Handbook", Version 2.0, JPL D-11007.
- Berry, P. A. M., R. Smith, and J. Benveniste. 2019. Altimeter Corrected Elevations, Version 2 (ACE2). Palisades, NY: NASA Socioeconomic Data and Applications Center (SEDAC). <https://doi.org/10.7927/H40G3H78> ; <https://sedac.ciesin.columbia.edu/data/set/dedc-ace-v2>
- Bonnefond, P., P. Exertier, O. Laurain, Y. Menard, A. Orsoni, E. Jeansou and G. Jan, 2002, "Absolute calibration of Jason-1 and TOPEX/POSEIDON altimeters in Corsica (abstract)", Jason-1/TOPEX/POSEIDON Science Working Team, New Orleans, LA, USA.
- Brenner, A. C., C. J. Koblinsky, and B. D. Beckley, 1990, A Preliminary Estimate of Geoid-Induced Variations in Repeat Orbit Satellite Altimeter Observations, *J. Geophys. Res.*, 95(c3), 3033-3040.
- Brown, S., 2009, A Novel Near-Land Radiometer Wet Path Delay Retrieval Algorithm: Application to the Jason-2/OSTM Advanced Microwave Radiometer", submitted to IEEE Trans. Geosci. Rem. Sens.
- Callahan, P. S., 1984, Ionospheric Variations affecting Altimeter Measurements: A brief synopsis *Marine Geodesy*, 8, 249-263.
- Cartwright, D. E. and R. J. Tayler, 1971, New computations of the tide-generating potential, *Geophys. J. R. Astr. Soc.*, 23, 45-74.
- Cartwright, D. E. and A. C. Edden, 1973, Corrected tables of tidal harmonics, *Geophys. J. R. Astr. Soc.*, 33, 253-264.
- Chambers et al., 1998, Reduction of geoid gradient error in ocean variability from satellite altimetry, *Marine Geodesy*, 21, 25-40.
- Chelton, D. B., J. C. Ries, B. J. Haines, L. L. Fu, and P. S. Callahan, 2001, "Satellite Altimetry", *Satellite Altimetry and Earth Sciences*, ed. L.L. Fu and A. Cazenave, pp. 1-131.
- Collard, F., 2005: Algorithmes de vent et période moyenne des vagues JASON à base de réseaux de neurons. BO-021-CLS-0407-RF, Boost Technologies, 33 pp.
- Cruz Pol, S. L., C. S. Ruf, and S. J. Keihm, 1998, Improved 20-32 GHz atmospheric absorption model, *Radio Science*.
- Desai S. , Wahr J., Beckley B., 2015, Revisiting the pole tide for and from satellite altimetry, *Journal of Geodesy* volume 89, pages1233-1243
- Desai S. D. and Ries J.C., 2017, "Conventional model update for rotational deformation," in Fall AGU Meeting, New Orleans, LA, 2017
- Gaspar, P., F. Ogor, P. Y. Le Traon and O. Z. Zanife, 1994, Estimating the sea state of the TOPEX and POSEIDON altimeters from crossover differences, *J. Geophys. Res.*, 99, 24981-24994.
- Gaspar, P., F. Ogor and C. Escoubes, 1996, Nouvelles calibration et analyse du biais d'état de mer des altimètres TOPEX et POSEIDON, Technical note 96/018 of CNES Contract 95/1523.
- Gourrion, J., Vandemark D., Bailey S., Chapron B., Gommenginger G. P., Challenor P. G., and Srokosz M. A., 2002: A two-parameter wind speed algorithm for Ku-band altimeters. *J. Atmos. Oceanic Technol.*, 19, 2030-2048
- Haines, B., D. Kubitschek, G. Born and S. Gill, 2002, "Monitoring Jason-1 and TOPEX/POSEIDON from an offshore platform: The Harvest experiment (abstract)", Jason-1/TOPEX/POSEIDON Science Working Team, New Orleans, LA, USA.
- Imel, D., 1994, Evaluation of the TOPEX dual-frequency Ionosphere correction, *J. Geophys. Res.*, 99 (c12), pp 24895-24906.



- Keihm, S. J., M. A. Janssen, and C. S. Ruf, 1995, TOPEX/POSEIDON microwave radiometer (TMR): III. Wet troposphere range correction algorithm and pre-launch error budget, *IEEE Trans. Geosci. Remote Sensing*, 33, 147-161.
- Labroue S., P. Gaspar, J. Dorandeu, O.Z. Zanife, F. Mertz, P. Vincent and D. Choquet, 2004: Non parametric estimates of the sea state bias for the Jason-1 radar altimeter. *Marine Geodesy* 27 (3-4), 453-481.
- Le Provost, C., 2001, "Ocean Tides", *Satellite Altimetry and Earth Sciences*, ed. L.L. Fu and A. Cazenave, pp. 267-303.
- Le Provost, C., F. Lyard, M. L. Genco, F. Lyard, P. Vincent, and P. Canceil, 1995, Spectroscopy of the world ocean tides from a finite element hydrodynamic model, *J. Geophys. Res.*, 99, 24777-24797.
- Lefèvre F., F. Lyard, C. Le Provost and E.J.O Shrama, Fes99 : a global tide finite element solution assimilating tide gauge and altimetric information, *J. Atm. Oceano. Tech.*, submitted, 2001.
- Lemoine, F. G. et al., 1998, The Development of the joint NASA GSFC and NIMA Geopotential Model EGM96, NASA/TP-1998-206861, 575 pp.
- Lillibridge, J., Scharroo, R., Abdalla, S., & Vandemark, D. , 2014: One-and two-dimensional wind speed models for ka-band altimetry, *Journal of Atmospheric and Oceanic Technology*, 31(3), 630-638. <http://doi.org/10.1175/JTECH-D-13-00167.1>
- Pavlis, N. and R. H. Rapp, 1990, The development of an isostatic gravitational model to degree 360 and its use in global gravity modeling, *Geophys. J. Int.*, 100, 369-378.
- Poisson et al. 2020, Classification des échos Jason-3, SALP-NT-MA-EA-23416-CLS, 2020,Mar.18
- Rapp, R. H. et al., 1991, Consideration of Permanent Tidal Deformation in the Orbit Determination and Data Analysis for the TOPEX/POSEIDON Mission, NASA Tech. Memorandum 100775, Goddard Space Flight Center, Greenbelt, MD.
- Rapp, R. H., Y. M. Wang, and N. K. Pavlis, 1991, The Ohio State 1991 geopotential and Sea Surface Topography Harmonic Coefficient Models, Rpt. 410, Dept. of Geodetic Science and Surveying, The Ohio State University, Columbus, OH.
- Ray, R. D., 1999, A global ocean tide model from TOPEX/POSEIDON altimetry: GOT99.2, NASA Tech. Memorandum 1999-209478, Goddard Space Flight Center, Greenbelt, MD.
- Ray R D and Ponte R M, 2003 Barometric tides from ECMWF operational analyses, *Annales Geophysicae*, 21: 1897-1910, 2003.
- Rio M.-H., F. Hernandez, 2004, A mean dynamic topography computed over the world ocean from altimetry, in situ measurements, and a geoid model, *J. Geophys. Res.*, 109, C12032.
- Rio, M.-H., Schaeffer, P., Lemoine, J.-M., Hernandez, F. (2005). "Estimation of the ocean Mean Dynamic Topography through the combination of altimetric data, in-situ measurements and GRACE geoid: From global to regional studies." Proceedings of the GOCINA international workshop, Luxembourg.
- Rio M.-H., A. Pascual, P.-M. Poulain, M. Menna, B. Barceló, and J. Tintoré, 2014, Computation of a new mean dynamic topography for the Mediterranean Sea from model outputs, altimeter measurements and oceanographic in situ data. *Ocean Science*.
- Rodriguez, E., Y. Kim, and J. M. Martin, 1992, The effect of small-wave modulation on the electromagnetic bias, *J. Geophys. Res.*, 97(C2), 2379-2389.
- Ruf, C., S. Keihm, B. Subramanya, and M. Janssen, 1994, TOPEX/POSEIDON microwave radiometer performance and in-flight calibration, *J. Geophys. Res.*, 99, 24915-24926.
- Saastamoinen, J., 1972: Atmospheric correction for the troposphere and stratosphere in radio ranging of satellites, *Geophys. Monogr.*, 15, American Geophysical Union, Washington D.C.



- Sandwell, D. T., and W. H. F. Smith, 2013 : Slope Correction for Ocean Radar Altimetry, Journal of Geodesy, DOI 10.1007/s00190-014-0720-1, 2013.
<http://topex.ucsd.edu/sandwell/publications/149.pdf>
ftp://topex.ucsd.edu/pub/global_VD_1min/DH.grd
- Smith, W. H. F. and D. T. Sandwell, 1994, Bathymetric prediction from dense satellite altimetry and sparse shipboard bathymetry, *J. Geophys. Res.*, 99, 21803-21824.
- Stacey, F. D., 1977, *Physics of the Earth*, second ed. J. Wiley, 414 pp.
- Stammer, D., C. Wunsch, and R. M. Ponte, 2000, De-aliasing of global high frequency barotropic motions in altimeter observations, *Geophys. Res. Lett.*, 27, 1175-1178.
- Tapley, B. D. et al., 1994, Accuracy Assessment of the Large Scale Dynamic Ocean Topography from TOPEX/POSEIDON Altimetry, *J. Geophys. Res.*, 99 (C12), 24, 605-24, 618.
- Tierney, C., J. Wahr, F. Bryan, and V. Zlotnicki, 2000, Short-period oceanic circulation: implications for satellite altimetry, *Geophys. Res. Lett.*, 27, 1255-1258.
- Thibaut P., Piras F., Roinard H., Guerou A., Boy F., Maraldi C., Bignalet-Cazalet F., Dibarboure G., Picot N., 2021 BENEFITS OF THE “ADAPTIVE RETRACKING SOLUTION” FOR THE JASON-3 GDR-F REPROCESSING CAMPAIGN, IGARSS 2021
- Tournadre, J., and J. C. Morland, 1998, The effects of rain on TOPEX/POSEIDON altimeter data, *IEEE Trans. Geosci. Remote Sensing*, 35, 1117-1135.
- Tran, N., D. Vandemark, S. Labroue, H. Feng, B. Chapron, H. L. Tolman, J. Lambin, and N. Picot, 2010 : “Sea state bias in altimeter sea level estimates determined by combining wave model and satellite data”, *J. Geophys. Res.*, 115, C03020, doi:10.1029/2009JC005534.
- Tran N., D. Vandemark, E.D. Zaron, P. Thibaut, G. Dibarboure, and N. Picot , 2019: “Assessing the effects of sea-state related errors on the precision of high-rate Jason-3 altimeter sea level data”, *Advances in Space Research / special issue “ 25 Years of Progress in Radar Altimetry”*, doi:10.1016/j.asr.2019.11.034
- Valladeau, G., Thibaut, P., Picard, B., Poisson, J. C., Tran, N., Picot, N., & Guillot, A., 2015: *Using SARAL/AltiKa to Improve Ka-band Altimeter Measurements for Coastal Zones, Hydrology and Ice: The PEACHI Prototype*, *Marine Geodesy*, 38, 124-142.
<http://doi.org/10.1080/01490419.2015.1020176>
- Watson, C., R. Coleman, N. White, J. Church and R. Govind, 2002, "In-situ calibration activities in Bass Strait, Australia (abstract)", Jason-1/TOPEX/POSEIDON Science Working Team, New Orleans, LA, USA.
- Witter, D. L., and D. B. Chelton, 1991, A Geosat altimeter wind speed algorithm and a method for altimeter wind speed algorithm development, *J. Geophys. Res.*, 96, 8853-8860.
- Wunsch, C., 1972, Bermuda sea level in relation to tides, weather and baroclinic fluctuations, *Rev. Geophys. Space Phys.*, 10, 1-49.
- Yi, Y., 1995, Determination of Gridded Mean Sea Surface from TOPEX, ERS-1 and GEOSAT Altimeter Data, Rpt. 434, Dept. of Geodetic Science and Surveying, The Ohio State University, Columbus, 9363-9368.
- Zaron E. D, 2019, Baroclinic tidal sea level from exact-repeat mission altimetry. *Journal of Physical Oceanography*, 49(1):193-210, 2019; "HRET_v8.1":
<http://web.cecs.pdx.edu/~zaron/pub/HRET.html>
- Zlotnicki, V., 1994, Correlated environmental corrections in TOPEX/POSEIDON, with a note on ionospheric accuracy, *J. Geophys. Res.*, 99, 24907-24914.



Annexe B - List of acronyms

AD	Applicable Document
AGC	Automatic Gain Control
AMR	Advanced Microwave Radiometer
AVISO	Archivage, Validation et Interprétation des données des Satellites Océanographiques
BRAT	Basic Radar Altimetry Toolbox
BUFR	B inary U niversal F orm for the R epresentation of Meteorological data
CLIVAR	Climate Variability and Predictability program
CLS	Collecte Localisation Satellites
CNES	Centre National d'Etudes Spatiales
DIODE	Détermination Immédiate d'Orbite par Doris Embarque
DORIS	Détermination d'Orbite et Radiopositionnement Intégrés par Satellite
DTM	Digital Terrain Model
ECMWF	European Center for Medium range Weather Forecasting
EGM	Earth Gravity Model
EM	ElectroMagnetic
EUMETSAT	European Organisation for the Exploitation of Meteorological Satellites
FES	Finite Element Solution
FFT	Fast Fourier Transform
GDR	Geophysical Data Records
GIM	Global Ionosphere Maps
GODAE	Global Ocean Data Assimilation Experiment
GPS	Global Positioning System
GTS	Global Telecommunications System
HF	High Frequency
IB	Inverse Barometer
IGDR	Interim Geophysical Data Records
JAXA	Japan Aerospace Exploration Agency
JGM	Joint Gravity Model
JPL	Jet Propulsion Laboratory
LPT	Light Particle Telescope
MDT	Mean Dynamic Topography
MLE	Maximum Likelihood Estimator
MSS	Mean Sea Surface
NASA	National Aeronautics and Space Administration
NetCDF	Network Common Data Form
NOAA	National Oceanic and Atmospheric Administration
NRT	Near Real Time
NWP	Numerical Weather Prediction
OGDR	Operational Geophysical Data Records
OSTM	Ocean Surface Topography Mission
OSU	Ohio State University
PO.DAAC	Physical Oceanography Distributed Active Archive Center
POD	Precision Orbit Determination
POE	Precision Orbit Ephemerides
PROTEUS	Plate Forme Reconfigurable pour l'Observation de la TERre, les telecommunications et les Utilisations Scientifiques
RD	Reference Document
RMS	Root Mean Square
RSS	Root Sum Square
SLA	Sea Level Anomaly
SLR	Satellite Laser Ranging
SSALTO	Segment Sol multimissions d'ALTimétrie, d'Orbitographie et de localisation



Jason-3 Products Handbook

Iss :2.1 - date : June 21^h , 2021



74

SSB	précise
SSH	Sea State Bias
SSHA	Sea Surface Height
SWH	Sea Surface Height Anomaly
T/P	Significant Wave Height
T2L2	Topex/Poseidon
TBC	Time Transfer by Laser Link
TBD	To be confirmed
TEC	To be defined
TRSR	Total Electron Content
UTC	Turbo Rogue Space Receiver
WMO	Universal Time Coordinated
	World Meteorological Organisation



Annexe C - Contacts

CNES

18, avenue Edouard Belin
F-31401 Toulouse Cedex 9

Web : www.cnes.fr

AVISO+ User Service Helpdesk:

8-10 rue Hermès
F-31520 Ramonville-St-Agne, France

Fax : +33 (0) 561 393 782
Web : www.aviso.altimetry.fr
e-mail : aviso@altimetry.fr

EUMETSAT

EUMETSAT Allee 1
D-64295 Darmstadt, Germany

Web : www.eumetsat.int

User Service Helpdesk:

Tel : +49 6151 807 366/377
Fax : +49 6151 807 379
e-mail : ops@eumetsat.int

NOAA

User Service Helpdesk:

Tel : +1 301-713-3277
e-mail : NODC.services@noaa.gov